University of Illinois at Urbana-Champaign

ACRC

Air Conditioning and Refrigeration Center A National Science Foundation/University Cooperative Research Center

Tribology of Protective Hard Coatings for Oil-Less Compressors

T. A. Solzak and A. A. Polycarpou

ACRC TR-243 June 2006

For additional information:

Air Conditioning and Refrigeration Center
University of Illinois
Mechanical & Industrial Engineering Dept.
1206 West Green Street
Urbana, IL 61801

(217) 333-3115

Prepared as part of ACRC Project #171
Tribology of Coatings for Oil-Less Compressors
A. A. Polycarpou, Principal Investigator

The Air Conditioning and Refrigeration Center was founded in 1988 with a grant from the estate of Richard W. Kritzer, the founder of Peerless of America Inc. A State of Illinois Technology Challenge Grant helped build the laboratory facilities. The ACRC receives continuing support from the Richard W. Kritzer Endowment and the National Science Foundation. The following organizations have also become sponsors of the Center.

Arçelik A. S.
Behr GmbH and Co.
Carrier Corporation
Cerro Flow Products, Inc.
Copeland Corporation
Daikin Industries, Ltd.
Danfoss A/S
Delphi Thermal and Interior
Embraco S. A.
General Motors Corporation
Hill PHOENIX
Hydro Aluminum Precision Tubing
Ingersoll-Rand/Climate Control
Lennox International, Inc.
LG Electronics, Inc.
Manitowoc Ice, Inc.
Modine Manufacturing Co.
Novelis Global Technology Centre
Parker Hannifin Corporation
Peerless of America, Inc.
Samsung Electronics Co., Ltd.
Sanden Corporation
Sanyo Electric Co., Ltd.
Tecumseh Products Company
Trane
Visteon Automotive Systems
Wieland-Werke, AG

For additional information:

Air Conditioning & Refrigeration Center
Mechanical & Industrial Engineering Dept.
University of Illinois
1206 West Green Street
Urbana, IL 61801

217 333 3115

Abstract

Compressors are being required to operate at increasingly severe conditions in order to increase efficiency, and with the transition from CFC to HFC and natural refrigerants, natural ferrous chloride layers on iron surfaces have been eliminated. To recover lost wear resistance with the transition to oil-less operation, greater protection is sought through the application of hard coatings with enhanced tribological properties.

Controlled shoe-on-disk experiments simulating the interface in a swashplate compressor were performed using a High Pressure Tribometer under unlubricated conditions. Specimens used for these experiments included 52100 steel shoes and coated aluminum A390-T6 disks. Coatings were provided by two leading manufacturers and consisted of two different single layer WC/C coatings (one from each manufacturer), multi-layer WC/C + DLC and multi-layer TiAlN + WC/C. To help increase load bearing ability on the relatively soft aluminum, a CrN underlayer was deposited on half of the disks. The performance of the coatings was evaluated using surface profilometry and scanning electron microscopy. In some cases, the CrN underlayer increased friction due to increased roughness, while it also significantly increased the load bearing capability in most applications. One of the CrN + WC/C multi-layered coatings exhibited friction coefficients similar to lubricated experiments with scuffing loads roughly ten times larger than uncoated, unlubricated tests.

Controlled, reciprocating pin-on-disk experiments imitating the wrist pin-connecting rod interface were also performed under unlubricated conditions. Specimens used for these experiments included coated, cylindrical 52100 steel wrist pins and uncoated cast iron disks. Coatings used were the same as those for the swashplate simulation tests but without the CrN underlayer. Analysis of experiments investigating temperature effects, frequency variation, and performance in various refrigerants including R134a, R410a, and R600a, was completed using scanning electron microscopy, energy dispersive x-ray microanalysis, and surface profilometry. It was found that steady-state friction coefficients decreased with increasing temperature while friction coefficients increased during the running-in period. Also, wear decreased from testing in room temperature up to 80°C and beyond that, increased due to unstable running-in. Tests conducted in R410a produced the lowest wear, while those in R600a had the lowest friction coefficients. Tests in R134a performed the worst, but better than tests conducted in dry nitrogen. Based on the research presented in this work, hard coatings have the potential to replace oil in future compressors.

Table of Contents

List of Figures

Page

List of Tables

Page

Chapter 1: Introduction

1.1 Research Overview

During the course of this research, the main objective was to conduct experiments to simulate compressors with the application of hard, protective coatings. Several coatings were obtained and deposited on materials relevant to swashplate and piston-type compressors, tested in a variety of conditions, analyzed, and ranked by performance.

1.2 Literature Review

The transition from chlorofluorocarbon (CFC) refrigerants to environmentally friendly refrigerants such as hydrofluorocarbons (HFC), hydrocarbons (HC), and CO_2 for use in compressors, has necessitated the quest for wear resistant and low friction materials and interfaces. Because of the absence of chlorine which forms ferrous chloride layers on iron surfaces, the contact pressure limits allowed by HFCs have decreased from those of CFCs [1-2]. Furthermore, interfaces must be able to withstand severe operating conditions caused by smaller clearances and increased speeds and loads of current and future compressors. Also, the state of lubrication in many compressor components is limited and usually in the boundary and mixed lubrication regimes [3]. Additionally, an interest in transitioning towards oil-less compressors is desired to eliminate the negative effects on the thermodynamic efficiencies of refrigeration cycles. Under these dry sliding conditions, one cannot rely on oxide formation and other surface reaction layers alone for enhanced tribological performance, and some form of protective coatings will be necessary.

In order to better interpret results from compressor simulation with coatings in a dry environment, previous research involving lubricated testing is provided as a basis for comparison. Significant tribological testing of compressor simulation has been performed, especially at the Air Conditioning and Refrigeration Center (ACRC) at the University of Illinois. Until recently, most of the testing has been conducted under step-loading or "scuffing" conditions with typical pin-on-disk or swashplate compressor configurations [4-6]. In these tests, sliding velocity was generally held constant while the load was increased at prescribed intervals until the interface failed due to scuffing. Also, the majority of interfaces have required lubrication to obtain anything close to representative loads found in a compressor.

1.2.1 Lubrication Testing with Metallic Interfaces

The most common test configurations have been the simulation of a swashplate compressor where a 52100 steel pin or shoe is in contact with an aluminum A390-T6 disk (shoe-on-disk) and general pin-on-disk testing with a flat pin in contact with a cast iron disk. In dry conditions, these interfaces are hardly able to withstand a normal load of 10 lbf (45 N) with friction coefficients greater than 0.5 in an R134a environment [7].

Fully submerged lubrication has typically allowed the highest scuffing loads and lowest friction coefficients with the contacting interface submerged in lubricant. Using the shoe-on-disk interface in a PAG/CO_2 environment at 200 psi, Demas was able to attain normal loads in excess of 700 lbf (3120 N) with scuffing experiments while maintaining friction coefficients less than 0.1 and as low as ~0.02 [6]. In the majority of this testing, however, measurable wear cannot be obtained unless high loads are applied for durations of an hour or more [8].

To simulate lubrication states manifested in extreme compressor conditions, starved lubrication tests were conducted. By combining refrigerant and a small amount of oil in a cylinder with which to pressurize the test chamber, a prescribed rate of oil addition can be controlled. Using this method, the scuffing load is reduced to 510 lbf for the shoe-on-disk interface [5]. Due to the initial lack of lubrication, a running-in period was observed with an initial friction coefficient of 0.13. However, once steady-state was reached, friction coefficients as low as 0.02 were again obtained. Due to the immiscibility of some lubricants and refrigerants, Demas established another method of lubrication by adding oil to a small absorbing medium which contacted the disk opposite the shoe on the wear track. Performance was slightly better than typical starved lubrication experiments with friction coefficients of 0.1 and scuffing loads of 600 lbf for both CO_2 and R134a refrigerants [6].

1.2.2 Tribology of Polymers

Cannaday studied the tribological performance of unfilled and blended polymers as possible alternatives for materials in compressors [7]. Traditional flat pin-on-disk testing was conducted with polymer pins and both cast iron and aluminum A390-T6 disks. Some of the major findings for both types were that performance in R134a was better than that in air, PTFE and PTFE blends had low friction but higher wear than others, and although transfer films on the disk are generally thought to decrease wear and/or lower friction, it was difficult to quantify. Material transfer was apparent to the naked eye, but difficult to quantify with profilometry and chemical analyses.

Both pure PEEK and polyimide performed similarly, having higher friction and lower wear than PTFE. Also, in step-loading tests with starved lubrication, PEEK and polyimide were found to perform better than metals, lending themselves to alternative materials for some bearing applications. For blended polymers, the trend was similar, but PEEK had consistently lower friction with no running-in period. Blends with PTFE or graphite exhibited lower friction but, PTFE blends still had high wear. In R134a and a load of 50 lbf, PEEK BG and PEEK w/carbon obtained friction coefficients of ~0.09 and little or no wear, while polyimide blends had slightly higher friction coefficients of ~0.17 and similar wear.

1.2.3 Tribology of Coatings

There is little published research on the application of hard coatings in compressors and simulated environments, and none was found to specifically investigate reciprocating motion such as that of a piston-type compressor. One publication sought to investigate the wear in rotary compressors with and without a TiN coating in a polyol ester (POE) lubricant and R410a environment [2]. The basic findings were that the addition of TiN to the vane surface improves the wear resistance over an uncoated vane and that there exists an optimal initial surface roughness at which load carrying capacity and wear can be improved. However, the known issues of TiN producing high friction and high wear on the opposing interface were not discussed as they were generally not an issue in the fully lubricated environment.

Another publication also studied compressors with several coatings in a POE/R407C environment [1]. TiN of different deposition conditions, TiAlN, WC/C, and diamond-like carbon (DLC) were deposited, and a vane that had undergone an ion nitriding surface treatment was also tested. Dry and lubricated tests were performed with the conclusion that the WC/C coating was the most suitable, showing both good wear and friction characteristics, likely due to a transfer film on the uncoated surface. Ion nitriding was deemed unsuitable for cyclic stresses found in

compressors. TiAlN was found to be unsuitable due to high wear while TiN produced high friction. The most surprising conclusion was that DLC produced high wear and scuffing failure in both dry and lubricated conditions, attributed to high hardness and corrosive wear. This result contradicts many sources that report some forms of DLC are not only capable of super low friction (< 0.01) but are almost always accompanied by low wear [9-12]. Kennedy et al. found that tests with DLC-coated hardened 4140 steel produced 200 times less wear than uncoated tests with contact pressures of 300-500 MPa while friction was reduced by almost five times [12]. The coating was beneficial in lubricated tests as well, exhibiting 50% lower friction and 75% less wear than uncoated tests.

1.2.4 Refrigerants

Little research has been conducted to directly compare the tribological performance of compressor interfaces in different refrigerant environments under dry conditions. Some of the most popular refrigerants currently are R134a, R410a, and R600a (isobutane) which is mostly used outside of the United States due to government regulations of the flammable gas, but has been shown to have good thermodynamic properties. Yoon et al. performed steel pin on aluminum disk tests in several different refrigerants and found slightly less wear on those in an R410a environment versus R134a [8]. However, these tests were fully lubricated, and performance may have been influenced by the lubricant composition. Similarly, Garland et al. performed aluminum pin on steel disk testing with different refrigerant/lubricant combinations [11]. Using the same lubricant, it was found that R134a had better wear but worse friction characteristics at room temperature. At a temperature of 110°C, the trend was reversed. However, R600a and R134a require different lubricants (typically mineral oil for R600a and POE for R134a) due to miscibility issues and using these combinations produced different trends. The point to be made is that no significant testing has been conducted to compare refrigerants in a dry environment, let alone with coatings.

1.3 Research Objectives

In this research, the use of hard coatings was investigated for use in swashplate and piston-type compressors. The coatings chosen were single-layer WC/C from two leading coatings manufacturers, and multi-layered coatings, WC/C + DLC and TiAlN + WC/C. These coatings were chosen for their advertised and widely known low friction characteristics, high relative hardness, low surface energy, and, therefore, expected reduced adhesive and abrasive wear. The areas of investigation presented are friction, wear, and scuffing characteristics for swashplate compressor simulation, while piston-type compressor simulation is used to study performance at different speeds, temperatures up to 120°C including the amplified effects of running-in at elevated temperatures, and performance in various refrigerants and inert environments.

Chapter 2: Experimental Procedures

2.1 High Pressure Tribometer

A specialized high pressure tribometer (HPT) was used in this study to perform controlled tribological experiments and evaluate friction and wear characteristics while simulating typical operating conditions found in air conditioning and refrigeration compressors. A photograph and schematic of the HPT are shown in Figures 2.1 and 2.2. It uses an upper rotating spindle to which the disk is attached and a stationary fixture that holds the lower specimen. A power screw mechanism adjusts the vertical position of the lower fixture to open or close the pressure chamber and apply a controlled normal load ranging from 10 lbf (45 N) to 1000 lbf (4450 N). The lower fixture is mounted to a 6-axis force transducer which measures the forces in the x, y, and z linear directions to calculate the coefficient of friction for eccentric contacts by dividing the resultant of the tangential forces by the normal force. For concentric contacts, frictional torque, Mz, is used to calculate the friction coefficient. Rotary or theta-axis control regulates upper spindle oscillation amplitude and frequency up to 5 Hz or produce unidirectional rotation speeds up to 2000 rpm.

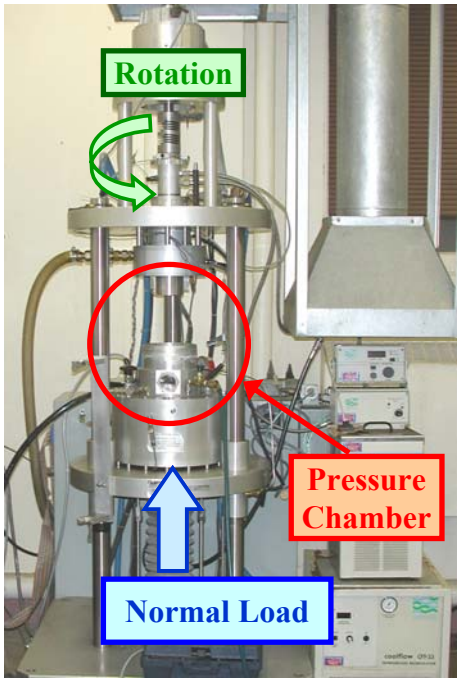

Figure 2.1: The High Pressure Tribometer

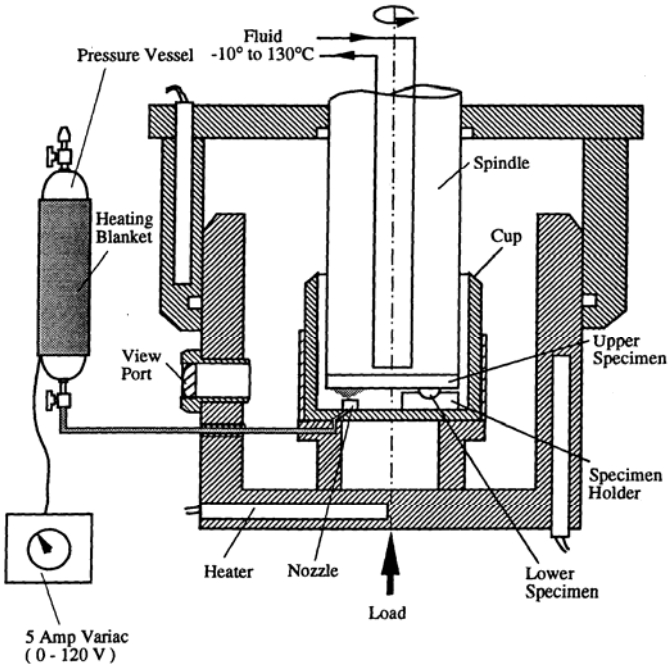

Figure 2.2: Schematic of HPT Pressure Chamber and Lubricant Supply System

The chamber temperature of the HPT can be varied from -20 to 120°C by pumping a heat transfer fluid through the upper spindle which is temperature regulated by an external unit. The chamber can also be vacuum evacuated and subsequently pressurized up to 250 psi (1.72 MPa). The HPT is computer controlled and acquires data including in-situ normal load, friction coefficient, and near contact temperature of the stationary specimen (approximately 2 mm below the surface with a miniature thermocouple) while exporting the data for analysis. Electrical contact resistance (ECR) can also be measured to determine the severity of the wear or lubrication state, but was not used in the data analysis due to apparatus problems, caused by issues with instrumentation and wiring,

for the majority of the experiments. A detailed description of the HPT can be found in Yoon [4], Patel [5], Demas [6], and Sheiretov [13].

2.2 Contact Geometry

2.2.1 Swashplate Compressor Simulation (Unidirectional)

The contact geometries used in this study were shoe-on-disk and pin-on-disk configurations. Shoe-on-disk testing has been conducted extensively in past ACRC projects for swashplate compressor simulation and consists of a 52100 steel shoe (Figure 2.3) that is allowed to self-align to form a flat contact with the disk (Figure 2.4). The self-aligning holder is depicted in Figure 2.5 and shows where the temperature and ECR measurements were made. An illustration of the contact is also displayed in Figure 2.6 while wear on an actual disk is exhibited in Figure 2.4 with a wear track diameter of 1.75" (44.5 mm). Although it appears that the shoe is flat, it is actually crowned with a dimple in the center causing higher contact pressure and wear initiation to occur where the central region of the shoe meets the disk. A cross section profile of the shoe is depicted in Figure 2.7.

Figure 2.3: 52100 Steel Shoe

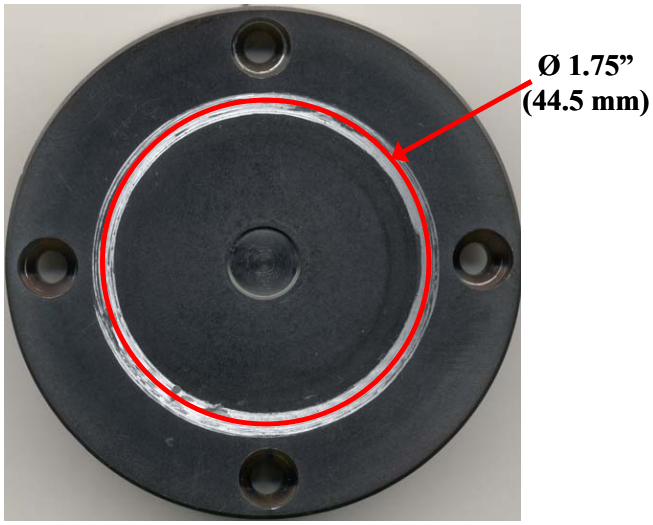

Figure 2.4: Worn WC/C-coated A390-T6 disk

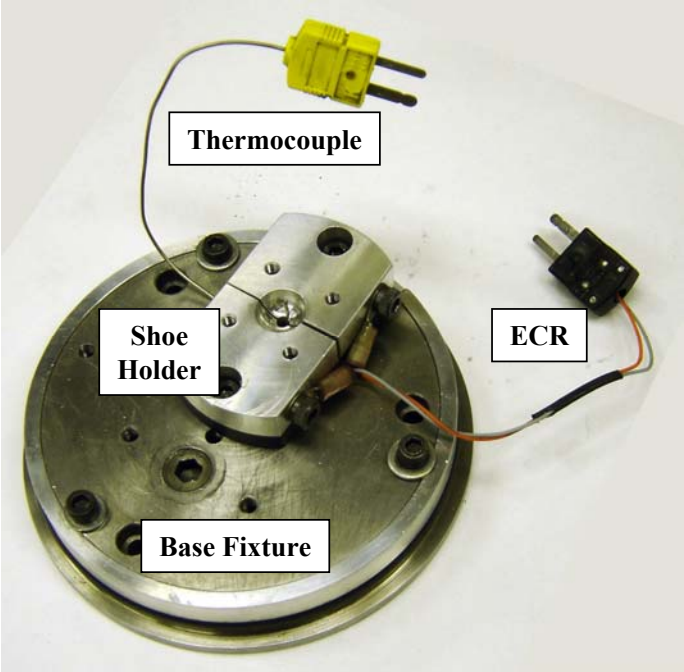

Figure 2.5: Self-aligning shoe holder with provisions for temperature and ECR measurements

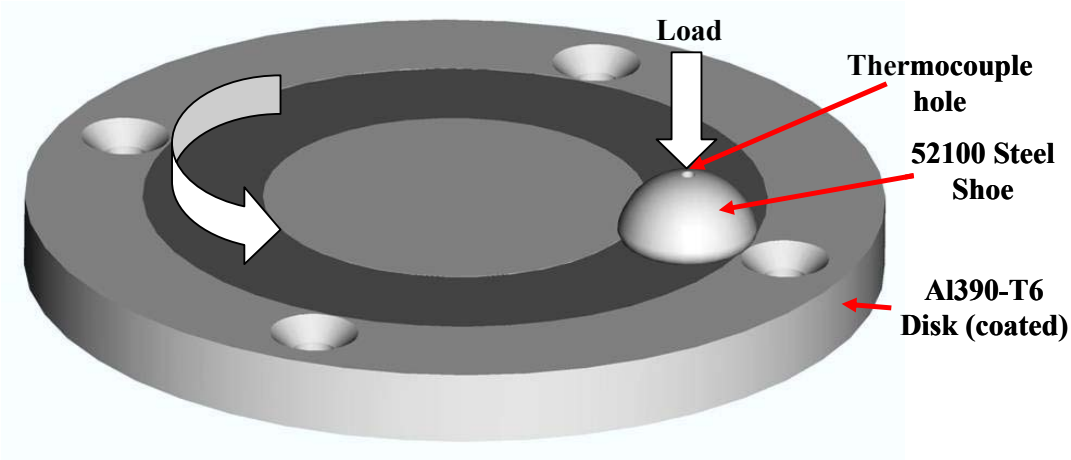

Figure 2.6: Illustration of shoe-on-disk contact and wear track

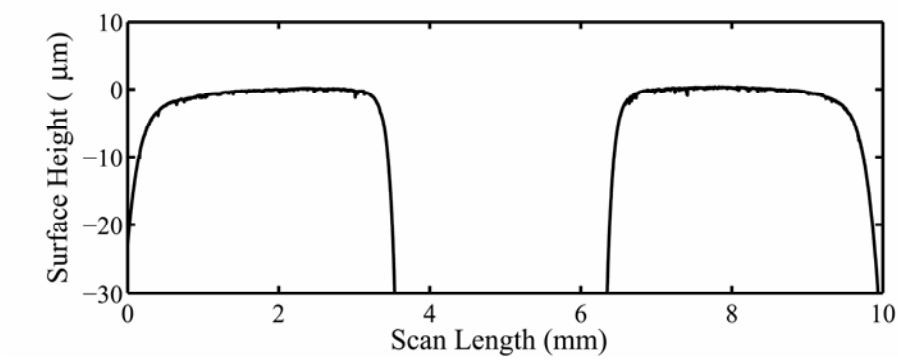

Figure 2.7: Cross section profile of 52100 steel shoe

2.2.2 Piston-type Compressor Simulation (Oscillatory Motion)

The emulation of the wrist pin/connecting rod interface (Figure 2.8) of a piston-type compressor was performed based on the equivalent contact pressure occurring on an actual connecting rod journal. Traditional pin-on-disk testing utilizes a cylindrical pin with a spherical top, usually a ball bearing, in contact with a flat disk. However, to achieve contact pressures relevant to piston-type compressors, relatively large contact radii on the order of 50 mm for the same load are needed necessitating custom pins. It proved difficult to attain a perfectly spherical surface due to manufacturing limitations, and many times a sharp point remained on the pin tip causing immediate severe wear. In this research, a new method was developed that used actual cylindrical wrist pins oriented to create a line contact as illustrated in Figure 2.9. Using this configuration, desired contact pressures were easily applied, and it is felt that test results were more applicable to piston-type compressors due to the similarity of the line contact. Pins were 8 mm in diameter and 8 mm long with a 1 mm diameter hole for miniature thermocouple insertion. They were produced from actual wrist pins that were cut to length and machined to have a flat seat (Figure 2.10). To accommodate this pin orientation, a special holder was designed which allows the pin to self-align (Figure 2.9(b)) to the disk surface ensuring a uniform contact pressure. The holder was similar to the shoe holder and is shown with provisions for temperature and ECR measurements in Figure 2.11. It was mounted such that a wear track diameter of 1.75" (44.5 mm) was attained, as depicted on the disk in Figure 2.12 that contains four tests. The disks for both piston-type and swashplate configurations are 3" (75 mm) in diameter and either 0.267" (6.8 mm) thick (cast iron) or 0.5" (12.7 mm) thick (aluminum). The exact dimensions of the pin and disks are given in Figures 2.13 and 2.14.

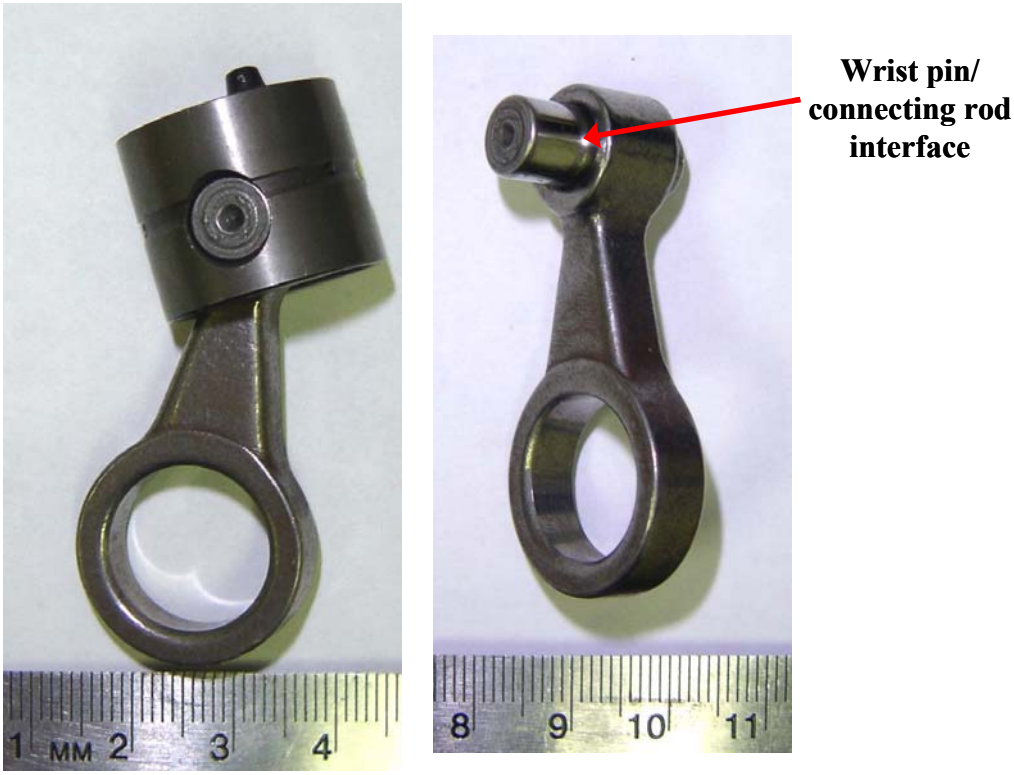

Figure 2.8: Piston assembly for a piston-type compressor indicating the wrist pin-connecting rod interface of interest.

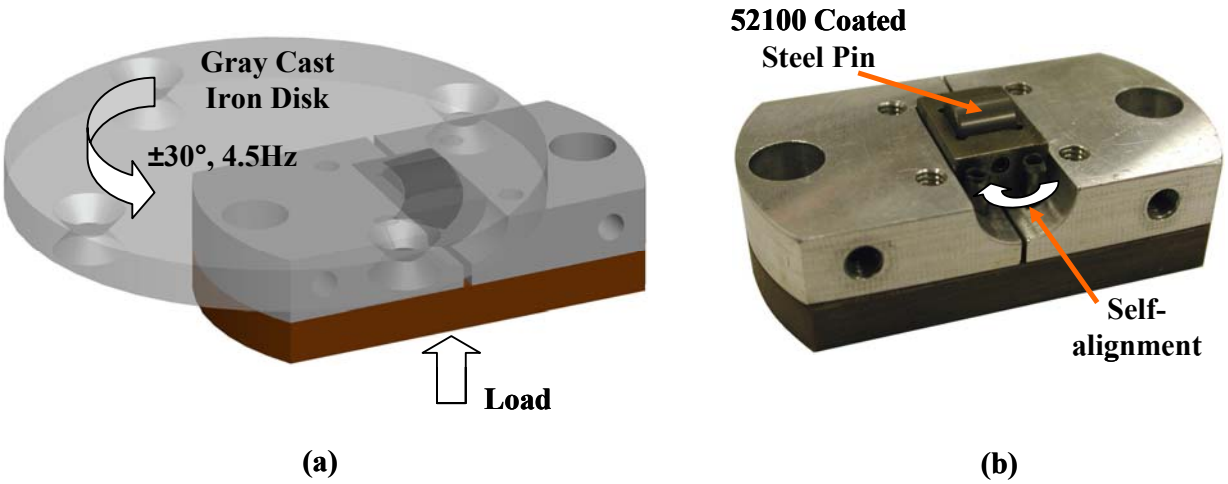

Figure 2.9: Illustration of (a) pin-on-disk contact and wear track and (b) self-alignment holder

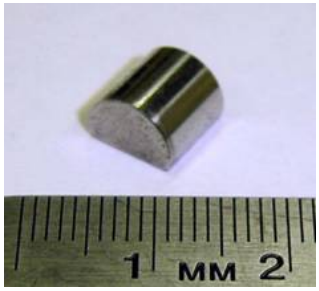

Figure 2.10: 52100 Steel pin test specimen machined from an actual wrist pin

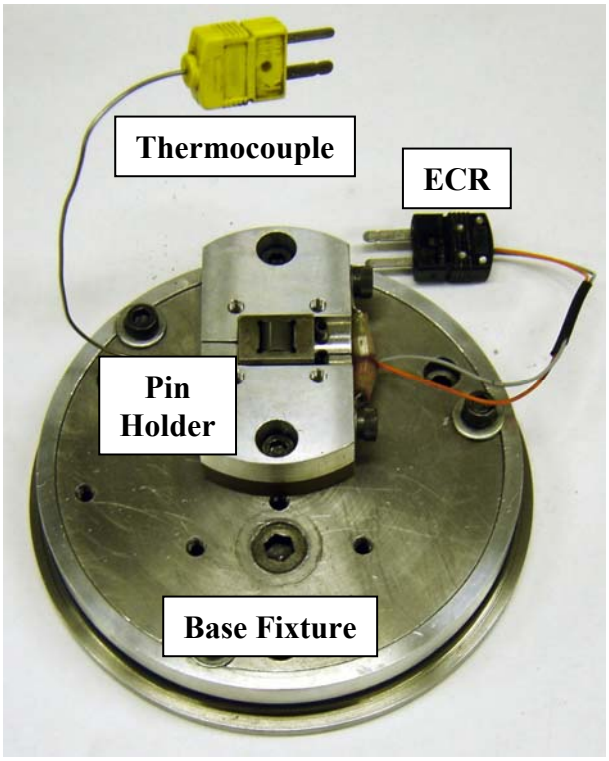

Figure 2.11: Self-aligning pin holder with provisions for temperature and ECR measurements for wrist pin testing

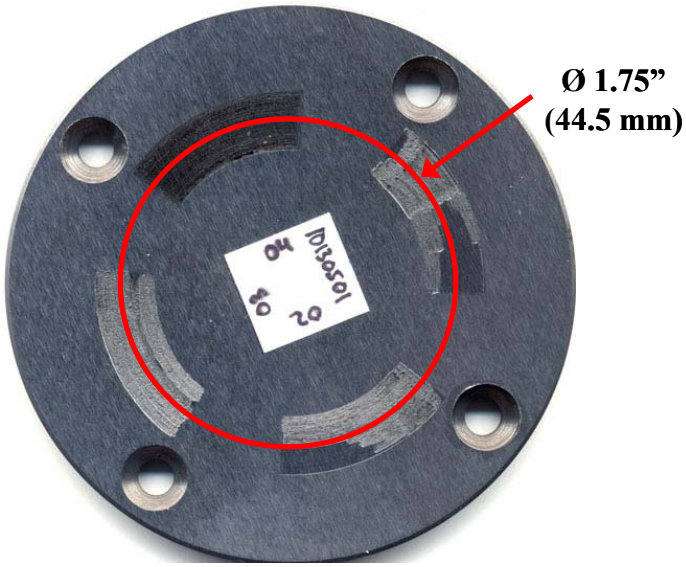

Figure 2.12: Gray cast iron disk with four tests

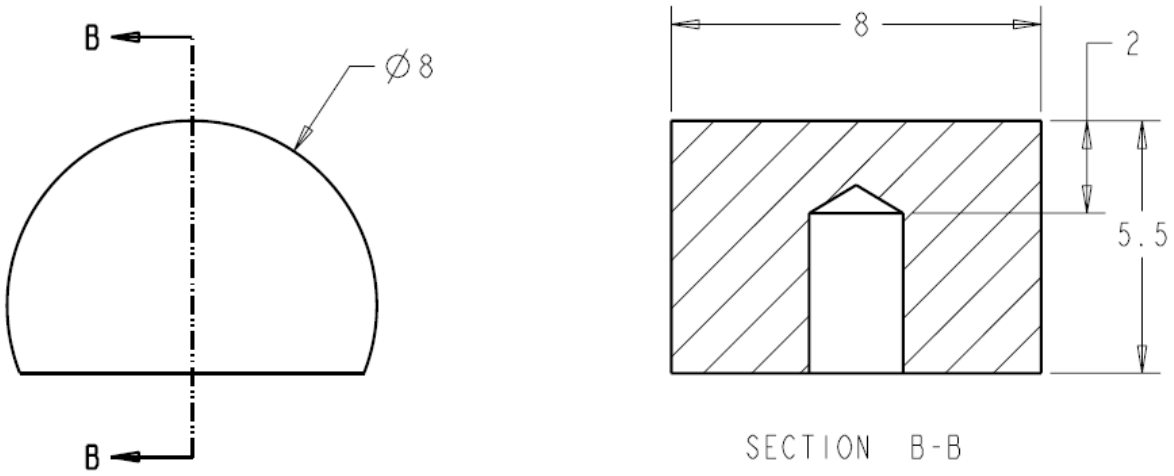

Figure 2.13: 52100 Steel cylindrical pin dimensions in millimeters (machined from wrist pin)

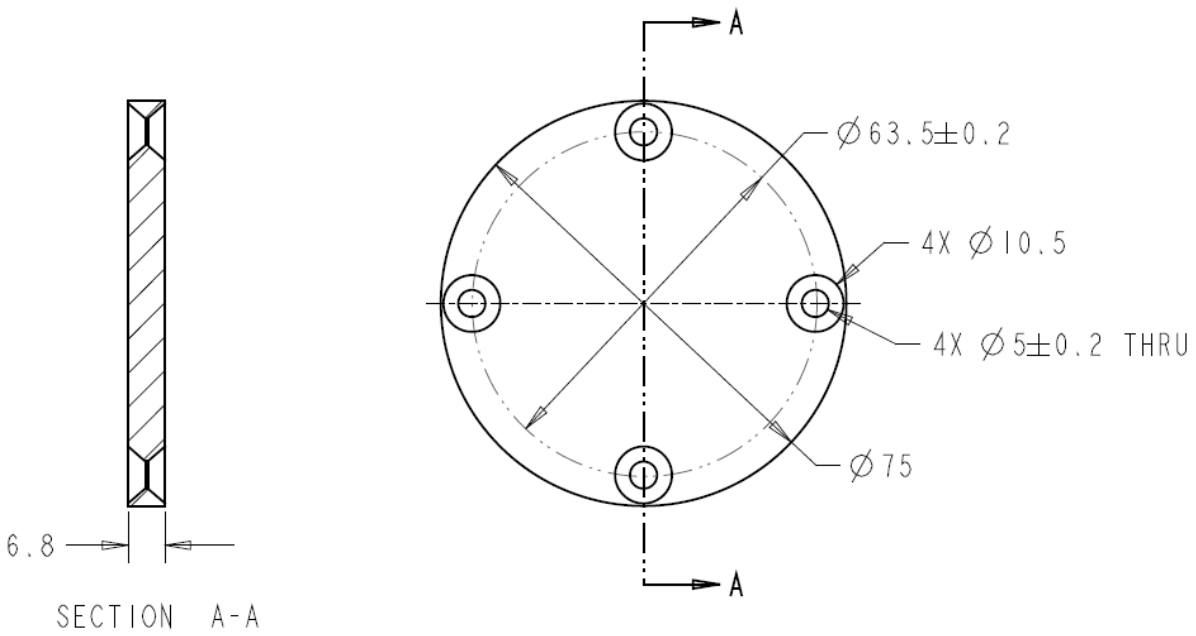

Figure 2.14: Cast iron and A390-T6 disk dimensions in millimeters (A390-T6 disk thickness is 12.7 mm)

2.3 Materials and Coatings

2.3.1 Swashplate Compressor Simulation

To simulate swashplate compressors, aluminum A390-T6 disks were used which are a cast Al-Si alloy obtained from Shotic Corp. and have an average hardness of 72 HRB [5]. The chemical compostion, obtained from MatWeb [14], is given in Table 2.1. As mentioned previously, the opposing interface was a SAE 52100 chrome steel shoe, which is the same part used in compressors and have a hardness of 62 HRC [14].

Table 2.1: Aluminum A390-T6 composition

	Element								
	Al	**Si**	**Cu**	**Fe**	**Mg**	**Mn**	**Ti**	**Zn**	**Other**
wt. %	75.2-79.6	16-18	4-5	< 0.5	0.45-0.65	< 0.1	< 0.2	< 0.1	< 0.2

It was decided to coat the aluminum disk as it is usually the area where the majority of wear occurs due to its low relative hardness compared to the 52100 steel shoe. Carbon based coatings were obtained from two leading manufacturers, due to their low friction and wear characteristics. Single-layer WC/C coatings from each company were acquired, and to differentiate between the two, they will be referred to as WC/C(A) and WC/C(B). Multi-layered WC/C + DLC and TiAlN + WC/C were also obtained. WC/C, an amorphous, hydrogenated metal-carbon coating (a-C:H:W), was chosen based on its successful application in areas where low friction ($\mu < 0.2$) is required. Although the performance of coatings usually varies due to adhesion layers used, deposition method, and surface roughness, according to the literature, WC/C has been found to perform similarly to harder, pure DLC (a-C:H, amorphous, hydrogenated carbon) coatings in terms of frictional characteristics and wear resistance [15]. Furthermore, the abrasive wear resistance of WC/C coatings has been found to be as high as TiN, a common coating

unsuitable for low friction applications with a friction coefficient of 0.6 or higher [16]. The good wear resistance is a result of the alternating tungsten carbide and amorphous carbon phases in layers a few atoms thick, which can also provide good running-in characteristics.

Multi-layered coatings are often used to increase tribological performance of the individual constituents. They can provide increased adhesion, increased load capacity, decreased surface stresses, and resistance to crack propagation [17]. WC/C + DLC was chosen due to the low friction and high wear resistance of each coating. However, it has also been shown that the DLC/WC pairing performs particularly well where cyclic loading is prevalent, such as gears and bearings [17], making it a good candidate for piston-type compressors. TiAlN + WC/C was also chosen for its advertised low friction and high wear resistance, but in all tests performed, caused instant failure at similar conditions to tests with other coatings, to be discussed in a later chapter. Due to the low relative hardness of the aluminum, it was suggested by the coatings manufacturers to investigate the effects of applying an additional hard underlayer of CrN to increase load capacity by bearing more of the load before deformation of the substrate occurs. A list of the coatings, substrates, and roughness of coated and uncoated samples used in this portion of testing is provided in Table 2.2 with their respective profiles scans in Figures 2.15-2.24. Coating thicknesses were not directly measured on the aluminum disks, but theoretically identical to those on the pins for the piston-type compressor simulation (Section 2.3.2), with the addition of a few micron thick CrN underlayer on some of the disks.

A third coating manufacturer, General Magnaplate, was also considered as a source of coatings, but due to time contstaints and the amount of coatings already obtained, their coatings were left for a future study. However, one of their coatings claims to have the lowest coefficient of friction in the world and some are polymer-based, lending themselves to softer substrates such as aluminum.

Table 2.2: Roughness of coatings and virgin test samples

Coated A390-T6 Disks		
Coating	**Ra (μm)**	**Rq (μm)**
WC/C(A)	0.72	0.93
CrN + WC/C(A)	1.67	2.50
WC/C(B)	0.19	0.24
CrN + WC/C(B)	0.44	0.54
TiAlN + WC/C	0.48	0.62
CrN + TiAlN + WC/C	1.57	2.35
WC/C + DLC	0.33	0.42
CrN + WC/C + DLC	0.43	0.54
Uncoated Samples		
A390-T6 Disk	0.41	0.52
52100 Steel Shoe	0.054	0.076

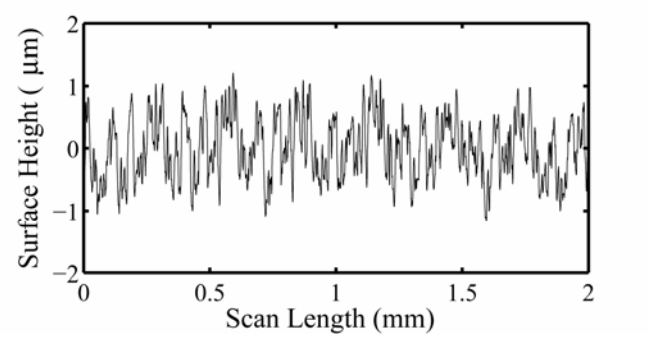

Figure 2.15: Uncoated A390-T6 disk roughness scan

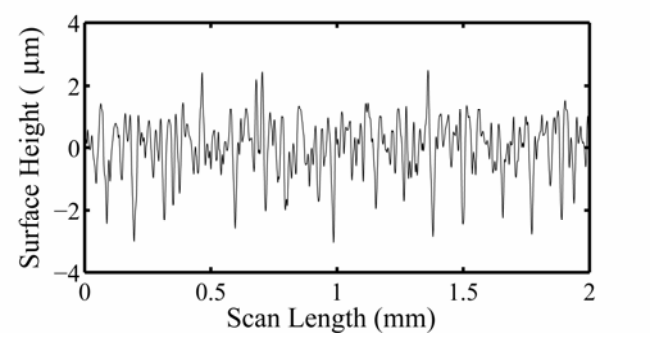

Figure 2.16: WC/C(A)-coated A390-T6 disk roughness scan

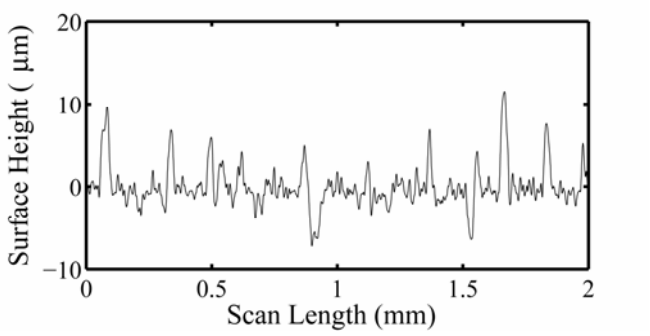

Figure 2.17: CrN + WC/C(A)-coated A390-T6 disk roughness scan

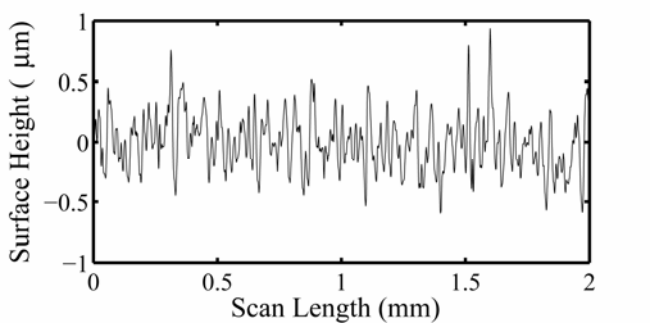

Figure 2.18: WC/C(B)-coated A390-T6 disk roughness scan

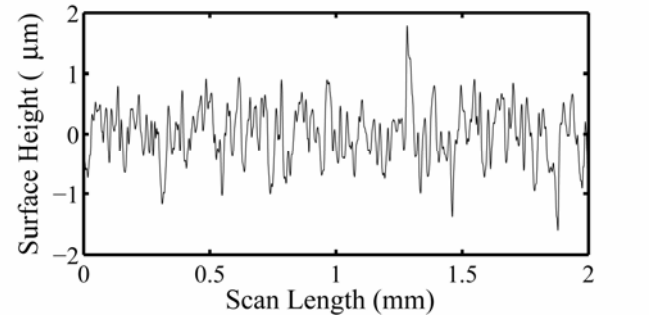

Figure 2.19: CrN + WC/C(B)-coated A390-T6 disk roughness scan

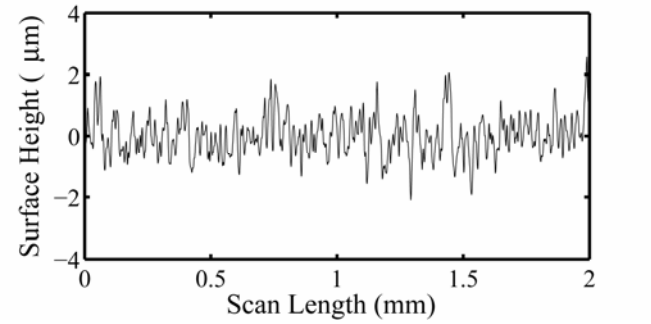

Figure 2.20: TiAlN + WC/C-coated A390-T6 disk roughness scan

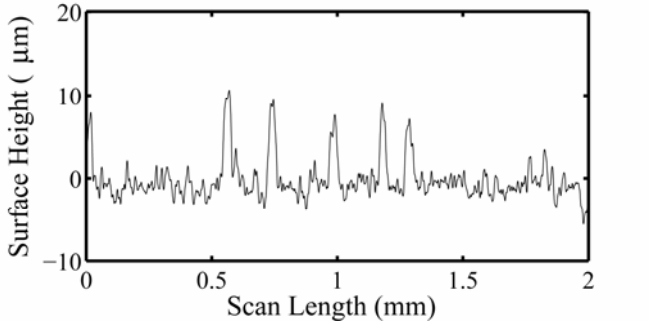

Figure 2.21: CrN + TiAlN + WC/C-coated A390-T6 disk roughness scan

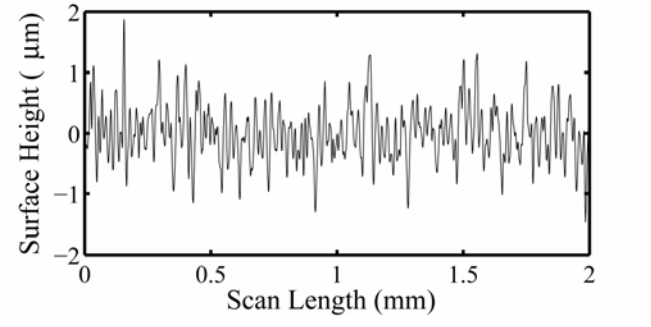

Figure 2.22: WC/C + DLC-coated A390-T6 disk roughness scan

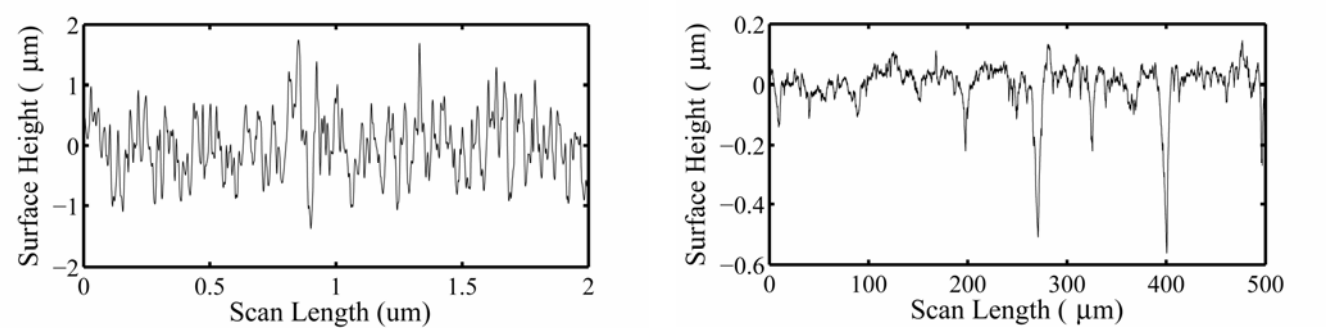

Figure 2.23: CrN + WC/C + DLC-coated A390-T6 disk roughness scan

Figure 2.24: 52100 steel shoe roughness scan

2.3.2 Piston-type Compressor Simulation

The substrates used for the piston-type compressor simulation were chosen to best simulate the wrist pin-connecting rod interface while at the same time remaining general for comparison to previous research as well as other types of compressors. The pins were produced from 52100 steel wrist pins that were modified to mount in the self-aligning holder (see Figure 2.9). Gray cast iron (Dura-Bar® G2) was chosen for the disk counter-surface as it is a commonly used material in compressor applications. Its chemical composition and mechanical properties are given in Table 2.3 [14].

Table 2.3: Gray cast iron composition

	Element									
	C	**Cr**	**Cu**	**Fe**	**Mn**	**P**	**S**	**Sb**	**Si**	**Sn**
wt. %	2.7-4.0	< 0.05	0.05-0.30	95	0.60-0.95	0.05-0.20	0.03-0.07	0.02-0.20	1.8-3.0	0.1-0.3

Unlike the shoe-on-disk testing, the harder 52100 steel pins were coated due to poor coating adhesion to gray cast iron as shown in Figure 2.25. Initially, the effects of coating one or both substrates were to be investigated, but poor adhesion dictated meant that only uncoated disks could be tested. Poor adhesion in gray cast iron stems from the soft, graphitic nature of the carbon content [18]. The same coatings were applied to the wrist pins as the aluminum disks, except without the CrN underlayer. A list of the coatings, substrates, and roughness of coated and uncoated samples used in this portion of testing is provided in Table 2.4 with their respective profiles scans in Figures 2.26-2.31. All coated samples have a ~0.5 µm thick Cr interlayer to promote adhesion, and the separate layers and thicknesses are displayed in Figure 2.32. TiAlN + WC/C is not shown due to poor performance, explained in later sections.

Figure 2.25: Cast iron disk with poor WC/C(A) coating adhesion

Table 2.4: Roughness of coatings and virgin test samples

Coated 52100 Steel Pins		
Coating	**Ra (nm)**	**Rq (nm)**
WC/C(A)	46	55
WC/C(B)	50	77
TiAlN + WC/C	278	433
WC/C + DLC	35	45
Uncoated Samples		
Cast Iron Disk	624	810
52100 Steel Pin	32	36

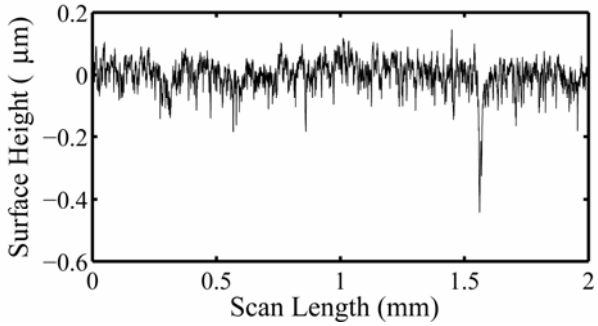

Figure 2.26: Uncoated pin roughness scan

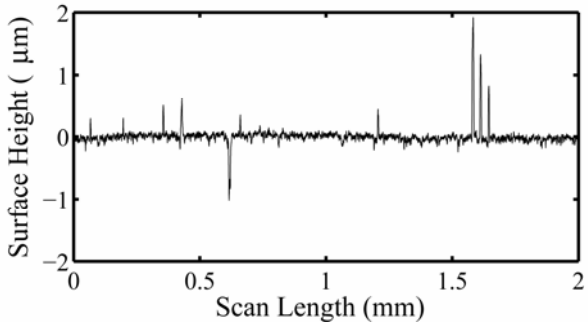

Figure 2.27: WC/C(A)-coated pin roughness scan

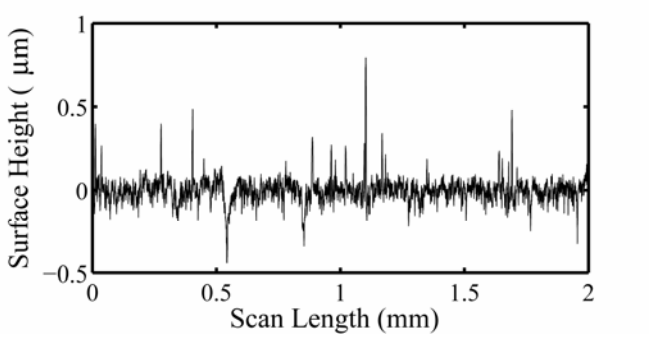

Figure 2.28: WC/C(B)-coated pin roughness scan

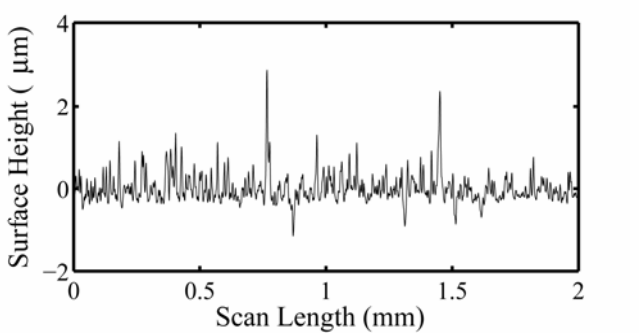

Figure 2.29: TiAlN + WC/C-coated pin roughness scan

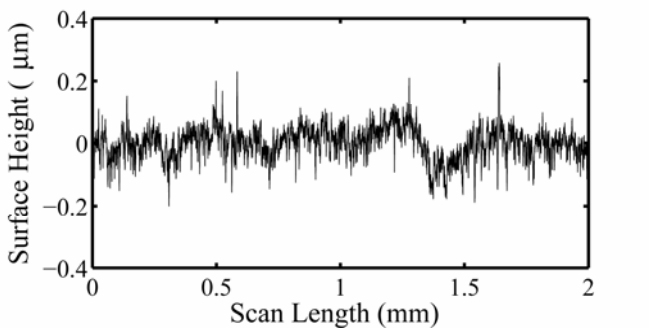

Figure 2.30: WC/C + DLC-coated pin roughness scan

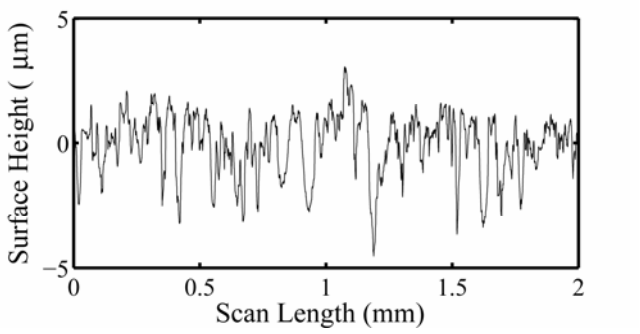

Figure 2.31: Gray cast iron disk roughness scan

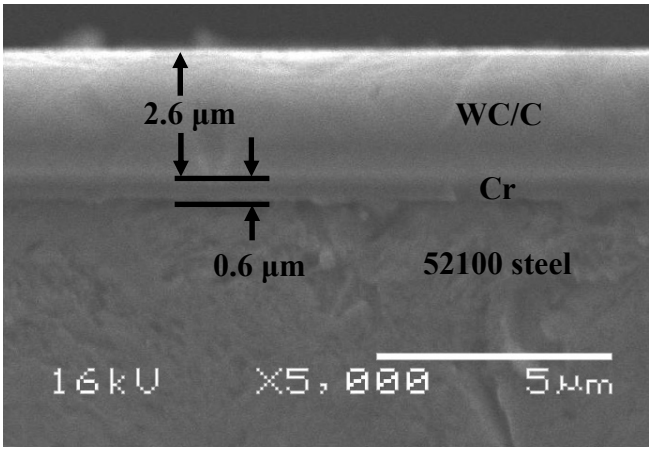

(a)

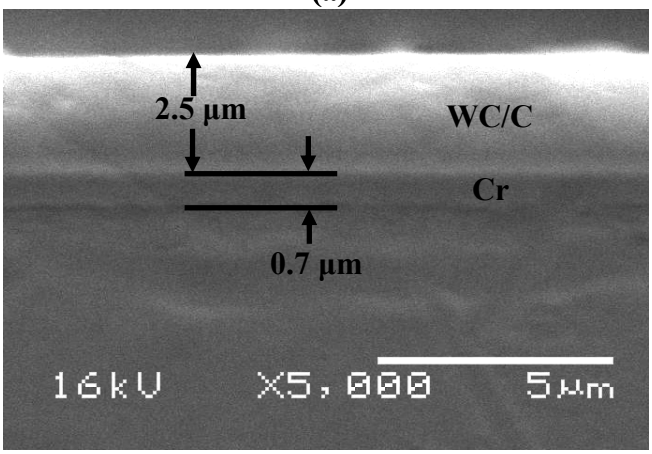

(b)

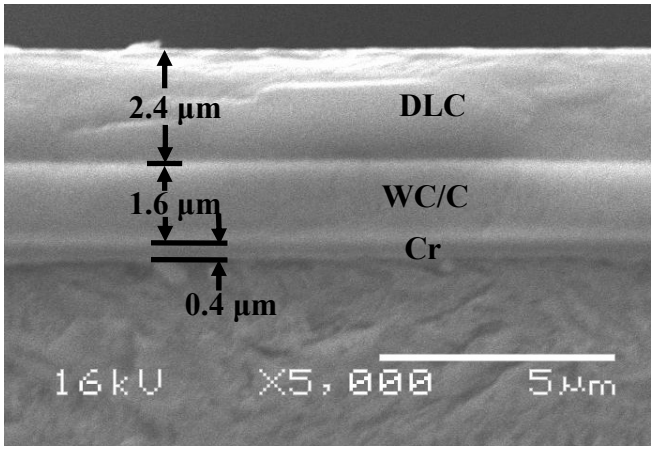

(c)

Figure 2.32: Cross-sectional SEM images of (a) WC/C(A), (b) WC/C(B), and (c) WC/C + DLC coated pins

2.3.3 Specimen Inventory

Only a limited amount of samples were available for coating and the number chosen for each coating was based on manufacturer's suggestions. A total of 28 A390-T6 disks were available and only able to be coated on one side due to cost issues. A total of 60 wrist pins were available as well as 60 cast iron disks. Also, only 10% of the

pins and shoes had thermocouple holes drilled. Again, this was a cost issue as the hard, bearing steel required two drill bits to finish one hole. Tables 2.5 and 2.6 list the quantity of all samples that were coated. Steel shoes were not coated and, thus, not listed.

Table 2.5: List of A390-T6 disks coated for swashplate compressor simulation

	WC/C(A)	CrN + WC/C(A)	TiAlN + WC/C	CrN + TiAlN + WC/C
# of Disks	4	3	4	3
	WC/C(B)	**CrN + WC/C(B)**	**WC/C + DLC**	**CrN + WC/C + DLC**
# of Disks	4	3	4	3

Table 2.6: List of 52100 steel pins and gray cast iron disks coated for piston-type compressor simulation

	WC/C(A)	WC/C(B)	TiAlN + WC/C	WC/C + DLC
# of Pins	20	10	10	10
# of Disks	10[1]	0	0	0

[1]Poor coating adhesion

2.3.4 Mechanical Properties

Nanoindentation measurements on coated and uncoated pins were performed to measure hardness and reduced Young's modulus values. A Hysitron TriboScope® nanoindenter was used in conjunction with a Berkovich tip to obtain contact depths of 50-200 nm and mechanical properties were determined using the Oliver and Pharr method [19]. The nanohardness and reduced modulus of bare 52100 steel were 12 GPa and 205 GPa, respectively, but higher than the bulk hardness of 7.3 GPa (converted from a hardness of 62 HRC). These values were assumed to be similar to those of the 52100 steel shoes. WC/C(A) hardness was similar at 10.5–12.5 GPa with a reduced modulus ranging from 90-125 GPa. While nanoindentation on WC/C(B) was not performed, it was assumed that it was similar to WC/C(A). The values for the WC/C + DLC coating were much higher with a hardness of 26 GPa and a reduced modulus of 200-220 GPa. The high values were expected as the indenter penetrated to a maximum depth of 200 nm, ensuring that only the properties of the top layer, in this case DLC, were quantified. The hardness values of all the substrates and coatings are summarized in Table 2.7 and also agreed with published values and manufacturer specifications [20-21]. The nanoindentation procedure and experiments are discussed further in Appendix A.

Table 2.7: Mechanical Properties of coatings and substrates

Material	Hardness (GPa)	Reduced Modulus (GPa)	HV (from mfr.)
Uncoated 52100 Steel	12	205	-
A390-T6[1]	4-6	70-100	-
Dura-Bar G2 gray cast iron	1.5-3[2]	124[3]	-
WC/C(A)	8-10	90-125	1500
WC/C(B)	-	-	1500
WC/C + DLC	26	200-220	2000-3500

[1]Obtained with a 90° cube corner tip [3], [2]Converted from Brinell hardness; [3]Bulk tensile modulus

2.4 Experimental Conditions

2.4.1 Set-up

Prior to all testing, the specimens were wiped clean with a towel and 2-propanol to remove large amounts of grease or rust inhibitor that was used to prevent oxidation on ferrous substrates. They were then ultrasonically cleaned in acetone for ten minutes, rinsed with 2-propanol, and dried with a blow dryer. It was found that if only ultrasonic cleaning was performed, residue or debris from machining was still present. A picture of the cleaning station in the Tribology Laboratory is shown in Figure 2.33.

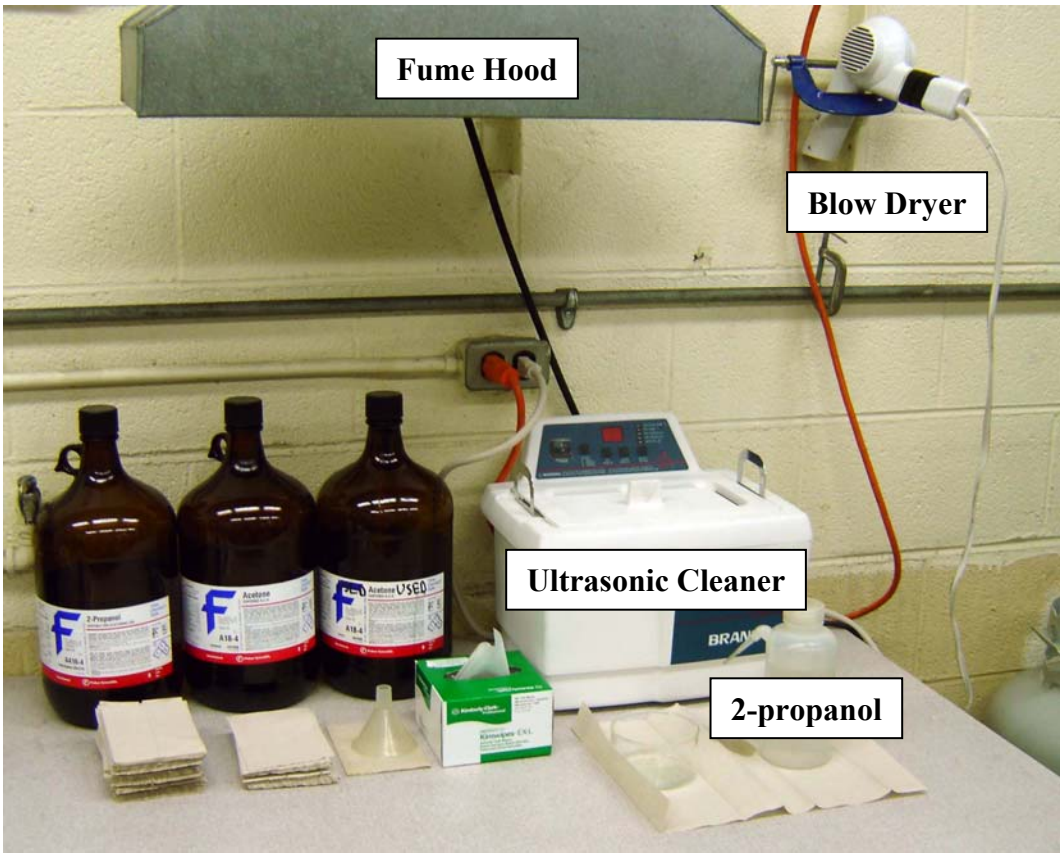

Figure 2.33: Cleaning station

The basic steps for the tests performed in this research are outlined below:

1. The desired chamber temperature is set on the external temperature control unit of the HPT.
2. The pin or shoe holder is attached to the lower base fixture which is then mounted inside the pressure chamber
3. The thermocouple and ECR wires are connected and positioned to avoid touching the upper spindle.
4. A clean shoe or pin is placed in the self-aligning holder using tweezers, and the disk is mounted to the upper spindle. Contact with the clean test surfaces is avoided.
5. The chamber is closed, vacuum evacuated to 0.1 Torr, and filled with refrigerant to the desired pressure.
6. The pin is brought into contact with the disk at an initial load of 10 lbf.
7. The test is initiated via the computer and data collection begins.

2.4.2 Swashplate Compressor Simulation

A limited number of tests were performed using the shoe-on-disk configuration due to the amount of coated disks available. All experiments were carried out at ambient temperature in refrigerant R134a at 25 psi. Rotation was unidirectional with a linear speed of 2.4 m/s. Both step-loading and constant load tests were performed in an effort to determine the maximum load carrying capability of the coating as well as quantify wear and wear rates. Step-loading tests were primarily performed with an initial load of 35 lbf with a 35 lbf increase every 30 seconds. It was found that the interface undergoes a running-in period with higher friction during which polishing and/or material transfer could occur possibly allowing the coating to perform better. For this reason, several tests were also conducted at a low load for a longer period of time before increasing to the final load to determine if the interface could sustain more extreme conditions.

Temperature was measured with a miniature thermocouple for a portion of this testing. This allowed observation of the near-contact temperature in anticipation of scuffing or coating failure which would be accompanied by a sharp temperature increase. An example of where temperature was an indicator of the onset of failure is shown in Figure 2.34. Note that after the increase in load, temperature increased dramatically, followed by a steady-state response, and finally, a sharp increase at coating failure. This figure also shows an example using an initial low load to wear-in the coating in an effort to achieve higher performance. Electrical contact resistance was also measured for the same reason, but due to difficulties in obtaining consistent measurements resulting from instrumentation problems, it was only considered qualitatively when "realistic" values were observed. Ideally, the ECR would exhibit a sharp decrease with scuffing. Figure 2.35 shows a case where ECR was a clear indicator of scuffing when the shoe and disk became friction welded to each other, decreasing the resistance between the two.

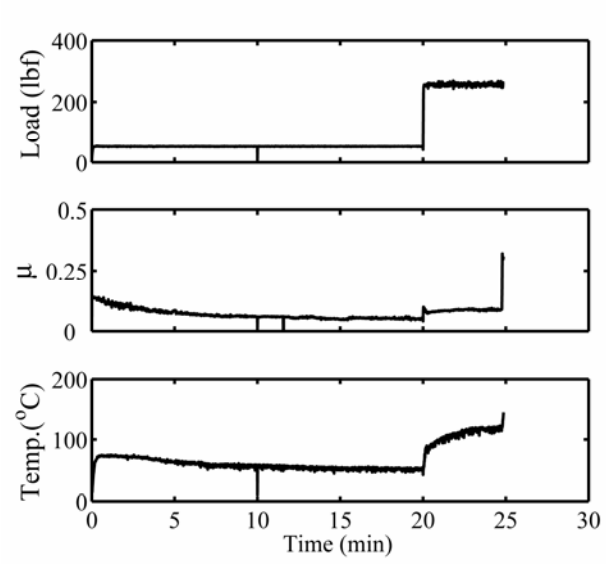

Figure 2.34: An example of temperature warning of scuffing failure with WC/C(A) coated disk in R134a @ 25 psi and ambient temperature

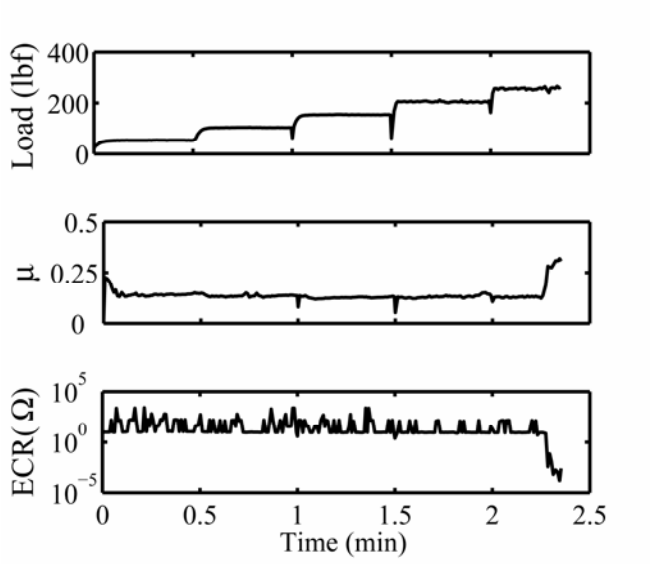

Figure 2.35: An example of ECR indicating scuffing failure with a CrN + WC/C + DLC coated disk in R134a @ 25 psi and ambient temperature

2.4.3 Piston-type Compressor Simulation

With the exception of a few preliminary experiments, all oscillatory experiments were performed under a constant normal load in order to evaluate wear and running-in. Due to the high wear resistance of the coatings, it was necessary to use higher contact pressures to obtain measurable wear with accelerated experiments. All tests were performed with an amplitude of 30 degrees, with an average wear track diameter of 1.75" (44.5 mm) in dry, unlubricated conditions for 21 minutes, unless otherwise noted.

Following all tests, wear and roughness were quantified using two profilometric scans on each disk and pin using a Tencor P-15 profilometer (see Appendix B for complete details). To precisely determine pin wear, the worn pin profile was subtracted from the original measurement of the cylindrical pin shape. The areas of the two scans were averaged and multiplied by the pin length to determine the wear volume. Figure 2.36 illustrates the scan directions on the pin and disk and method of wear quantification.

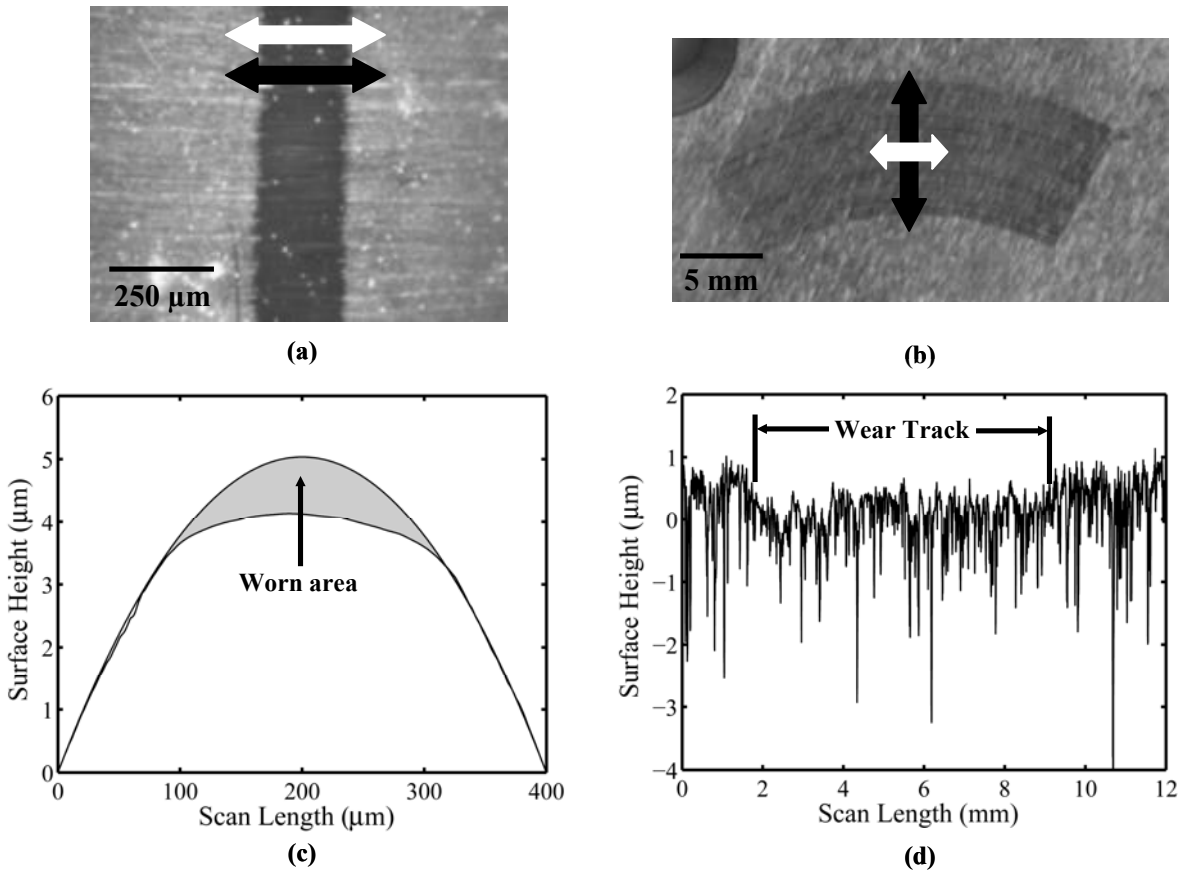

Figure 2.36: Images and profilometric scans of typical worn (a) pin and (b) disk. The white arrows on the pin micrograph denote the scan directions while the black arrows indicate the sliding direction.

2.4.3.1 Preliminary Experiments

As a baseline, uncoated experiments were performed first at a lower normal load of 45 lbf (200 N) for 10 minutes, the highest load attainable before premature scuffing failure, as shown in Figure 2.37. Preliminary testing with coatings was conducted at ambient temperature in R134a at 25 psi with a frequency of 4.5 Hz to determine a suitable normal load at which to conduct subsequent tests. Extremely high contact pressures were attainable, much higher than those present in a piston-type compressor. To demonstrate the effectiveness of the hard coatings, though, these results will be presented. Constant load experiments were performed with normal loads up to 300 lbf (1336 N), while a single step-loading test was performed with a maximum load of 750 lbf (3341 N) for an initial Hertzian contact pressure of 1.7 GPa, assuming elastic contact.

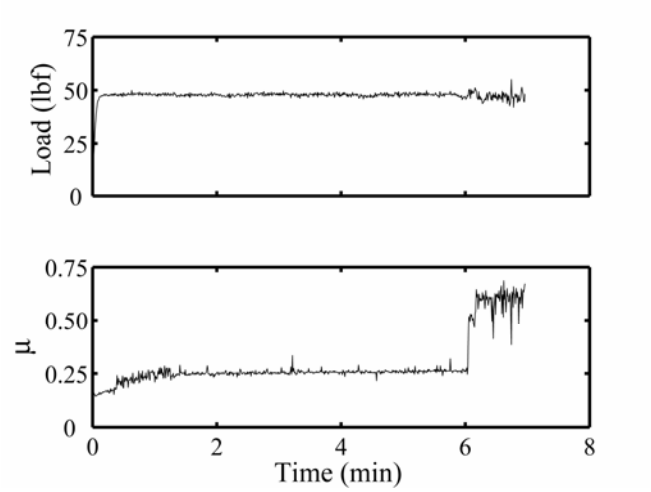

Figure 2.37: Uncoated pin-on-disk experiment exhibiting scuffing failure

2.4.3.2 Temperature Variation

Tests to investigate the effects of temperature variation were performed for all coatings with durations of 21 minutes. These times provided measurable wear from which performance distinction could be made without observing scuffing failures. For the first minute of each test, the normal load was set to half that of the remaining test load to aid running-in. In the absence of this initial lower load at the beginning of the running-in process, several immediate coating failures had occurred, as seen with WC/C(A) at just over 100 lbf (445 N) in Figure 2.38. The temperatures studied ranged from ambient (23°C) to 120°C.

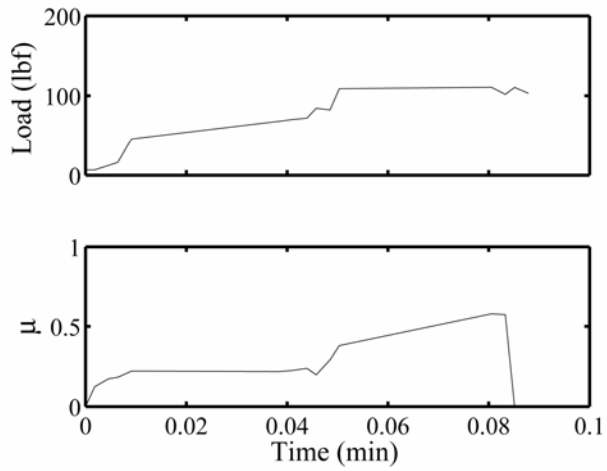

Figure 2.38: Example of immediate coating failure with WC/C(A)

Most tests were performed at a normal load of 100 lbf to quantify wear. At chamber temperatures above 60°C, a progressively increasing running-in period was observed where friction coefficients of up to 0.4 were measured, and to study this behavior, WC/C(A) was tested at 120°C and 50 lbf for 5, 10, and 21 minutes. A lower normal load was necessary due to immediate failure of WC/C(A) at 100 lbf and 120°C. Following this testing, 4 mm long roughness scans were completed on both the pin and disk to correlate roughness to the running-in process.

2.4.3.3 Refrigerant Variation

This group of testing aimed to determine how different refrigerants affected coating performance. WC/C + DLC, thought to be the highest performing to this point, was evaluated in R134a, R410a, and R600a while baseline tests were conducted in N_2. The chamber pressure was 25 psi for all environments to obtain the same number of refrigerant molecules present (according to the ideal gas law). These experiments were all performed at ambient temperature with a frequency of 4.5 Hz and a normal load of 100 lbf (445 N).

2.4.3.4 Oscillation Frequency Variation

The effects of speed on friction and wear were studied with frequencies of 3 Hz and 4.5 Hz to produce average linear speeds of 0.14 m/s and 0.21 m/s, respectively. Similar to other test groups, the normal load was set at 50 lbf (223 N) for the first minute and 100 lbf (445 N) thereafter. The test environment was at ambient temperature with R134a at 25 psi. To correctly correlate tests at different frequencies, the number of cycles was kept the same to achieve the same sliding distance.

Chapter 3: Results and Discussion

3.1 Swashplate Compressor Simulation

3.1.1 Preliminary Testing

Cannaday found that the friction coefficient of uncoated 52100 steel on an aluminum disk was unstable [7]. Figure 3.1 shows a 10 minute test at a load of ~15 lbf with a friction coefficient that is initially around 0.5, but begins to fluctuate soon after. Also, temperature was continuously rising through the duration of the test. The contact geometry was different than typical swashplate compressor testing with a flat 6.35 mm diameter pin; nevertheless, high adhesive friction of the two materials was exhibited. This test is shown as a baseline for coated tests.

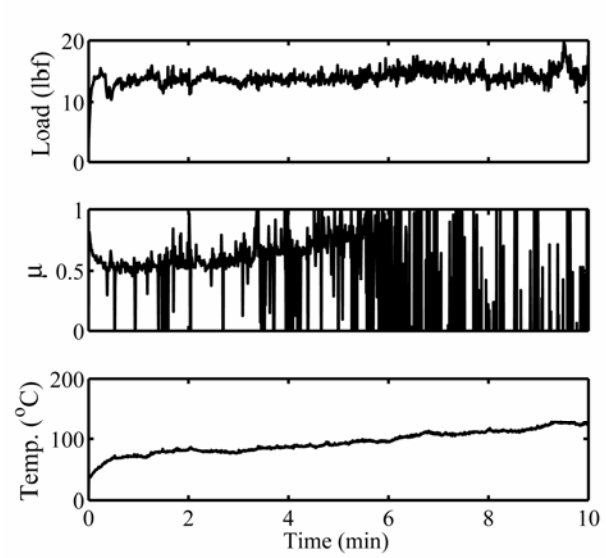

Figure 3.1: HPT data for a flat pin-on-disk test with no lubrication or coating [7]

During the preliminary experiments, it was immediately found that the TiAlN + WC/C coating was unsuitable for this application. Figure 3.2 shows the HPT data from one experiment, and although the friction coefficient is low relative to the uncoated experiment, the coating has completely worn through as shown in the micrograph in Figure 3.3 and accompanying wear scan in Figure 3.4. A cross section SEM image of a virgin TiAlN + WC/C coating on the aluminum (Figure 3.5) shows a subsurface crack which may have been caused by high residual stresses of the TiAlN underlayer. Figure 3.6 shows delamintation of a virgin TiAlN + WC/C coating which suggests that this particular coating has poor adhesion to A390-T6. It is interesting that the friction is still stable compared to the uncoated test due to the embedding of coating particles within the aluminum, exhibited in Figure 3.3.2. TiAlN + WC/C was eliminated from further testing, but it is important to note that it is possible that this multi-layered coating could perform better if it was optimized for the specific substrate.

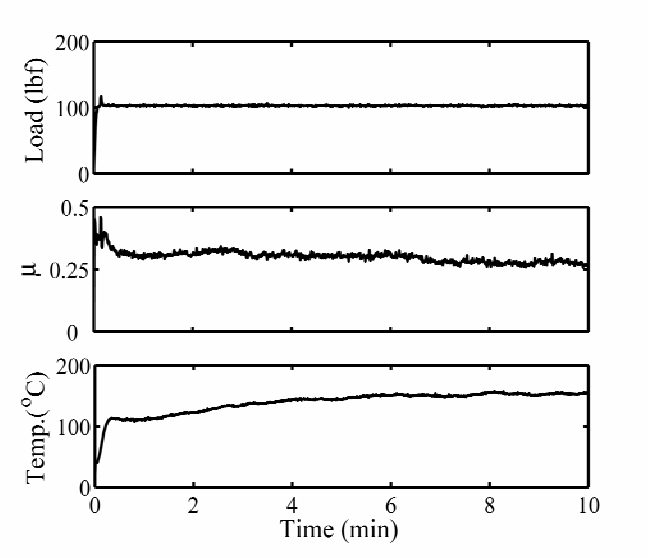

Figure 3.2: HPT data of TiAlN + WC/C -coated disk

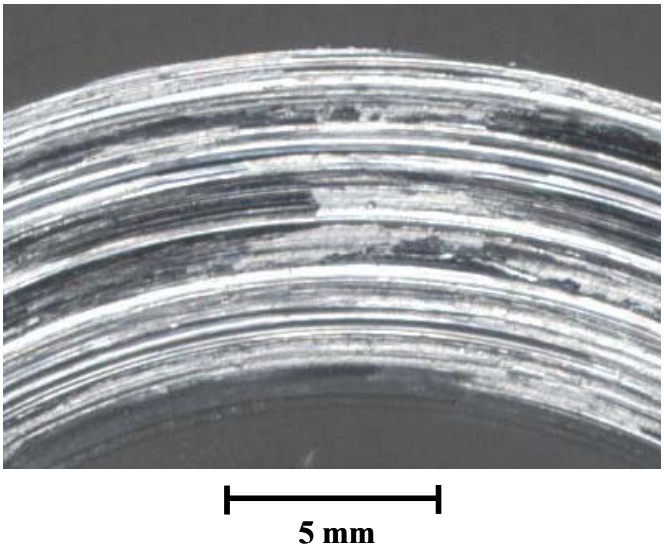

Figure 3.3: Wear scar of a failed TiAlN + WC/C-coated disk

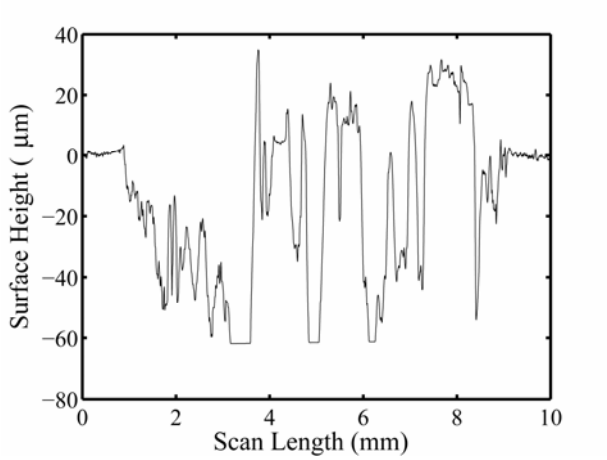

Figure 3.4: Profile scan of scuffed TiAlN + WC/C-coated disk

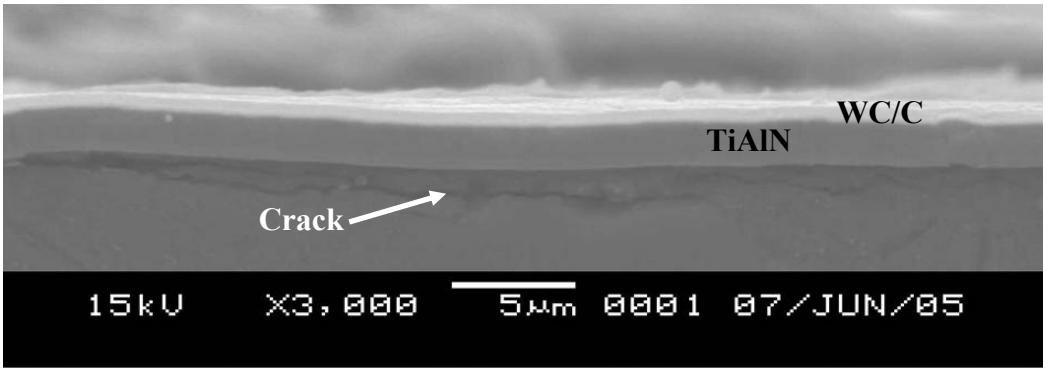

Figure 3.5: Cross-sectional SEM image of a virgin TiAlN + WC/C-coated disk showing subsurface cracks

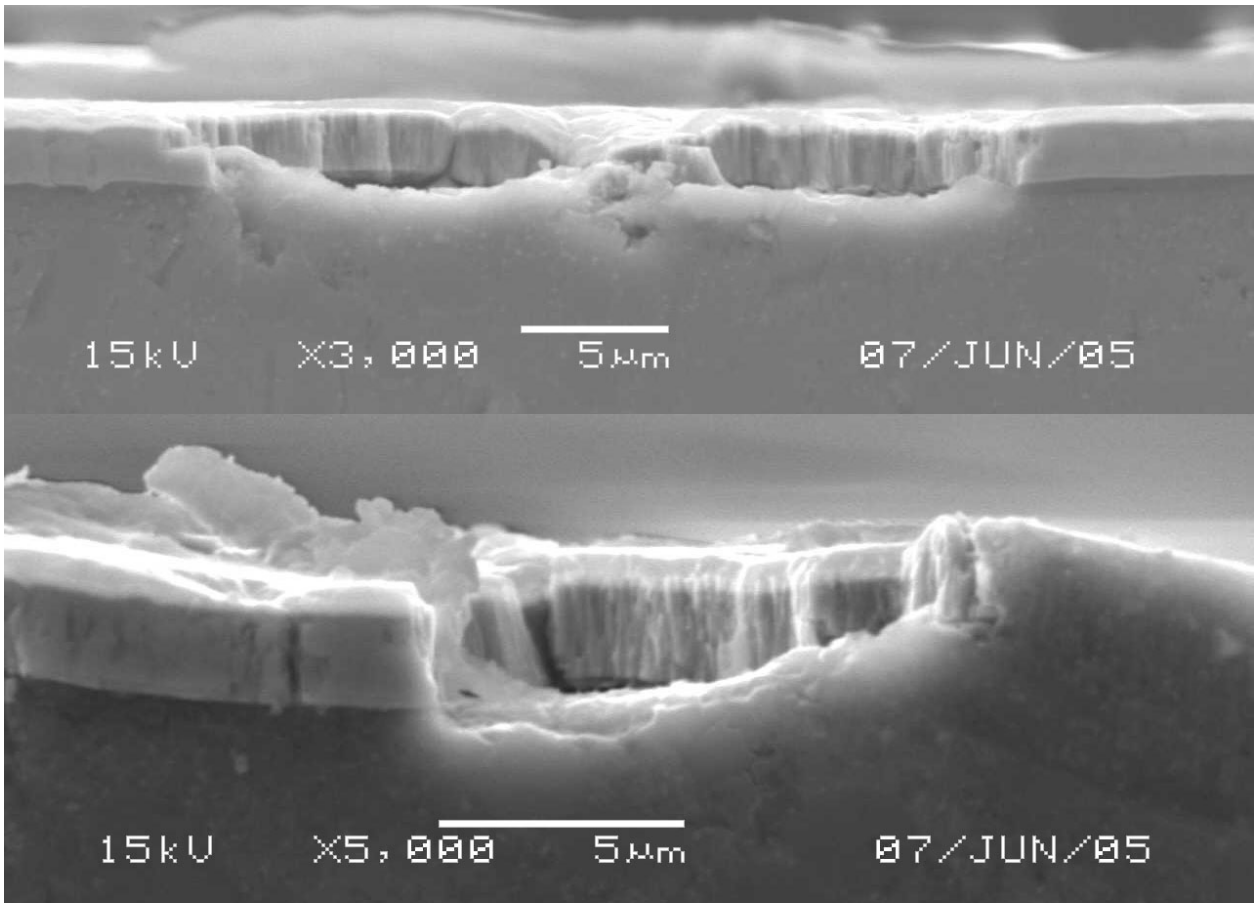

Figure 3.6: Cross-sectional SEM images of a virgin TiAlN + WC/C-coated disk showing delamination

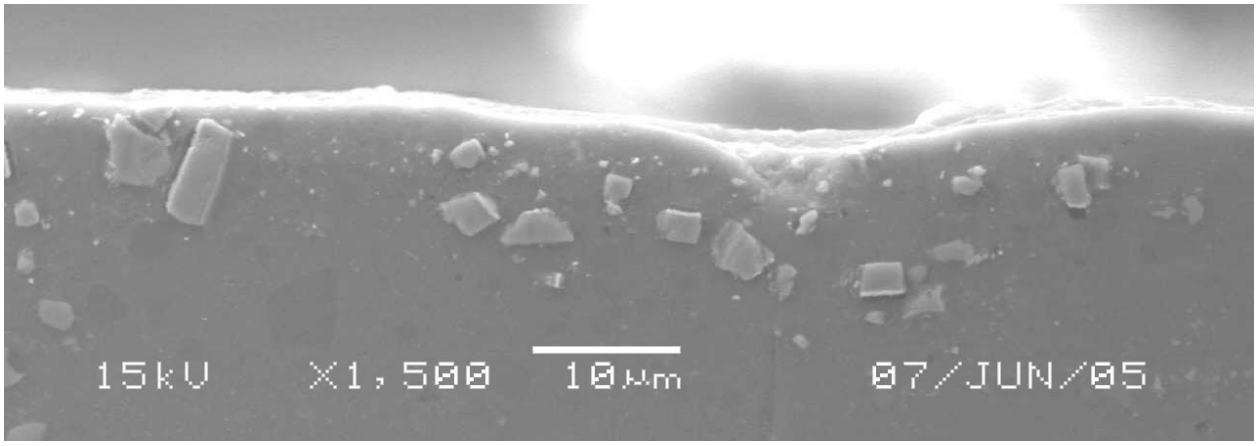

Figure 3.7: Embedding of coating particles in a scuffed TiAlN + WC/C-coated disk

3.1.2 Friction and Scuffing Experiments

In an effort to quantify wear on constant load tests, profilometric scans of the disk wear track were performed. It was difficult to distinguish wear from roughness on the disk, though, as mostly polishing occurred. Despite this difficulty in preliminary testing, a series of tests was performed with WC/C(A) at successively higher loads using the same disk with a new shoe each time to try and produce wear and investigate effects of transfer

films. After each test, only polishing was observed on the coating surface while the softer WC/C(A) (versus 52100 steel) formed a transfer film on the shoe, displayed in Figure 3.8. Transfer films have been shown to be a key ingredient to low friction in the literature [9-12], but seemed to have little or no effect in these tests. Table 3.1 lists the friction coefficients obtained with each load showing little variation except that it decreased slightly with higher loads. It became apparent through these tests and those explained next, that without extremely long tests, no measurable wear will be obtained. In general, with coated aluminum, the scuffing occurs due to the soft substrate and poor load support causing coating fracture.

Figure 3.8: WC/C(A) transfer film formed on 52100 steel shoe

Table 3.1: Results of successively higher loads on WC/C(A) coated disk

Load (lbf)	Duration (min.)	Friction Coeff., μ
40	10	0.13
75	10	0.11
100	10	0.13
150	10	0.11
200	10	0.07
250	4.33	0.09

Due to the difficulty of wear quantification in constant load tests, step-loading tests were performed until scuffing occurred to observe friction coefficients at different loads as well as determine the load bearing capability of the coatings. WC/C(B) and WC/C + DLC without a CrN underlayer appeared to be very inconsistent. A coating may be able to support a 250 lbf load in one test and scuff instantly at 35 lbf in the next test as shown with data from two tests in Figure 3.9. It is unknown whether this was due to differences in coating thicknesses or if the scuff marks and light scratches observed after shipping initiated scuffing. WC/C(A) disks, however, were shipped using the same method, had little or no scuff marks, and performed relatively consistently. As a result of the quality of WC/C(B), all step-loading tests starting at 35 lbf scuffed before the first load step. Only scuffing tests starting at 50 lbf with longer step durations were performed successfully and are presented later.

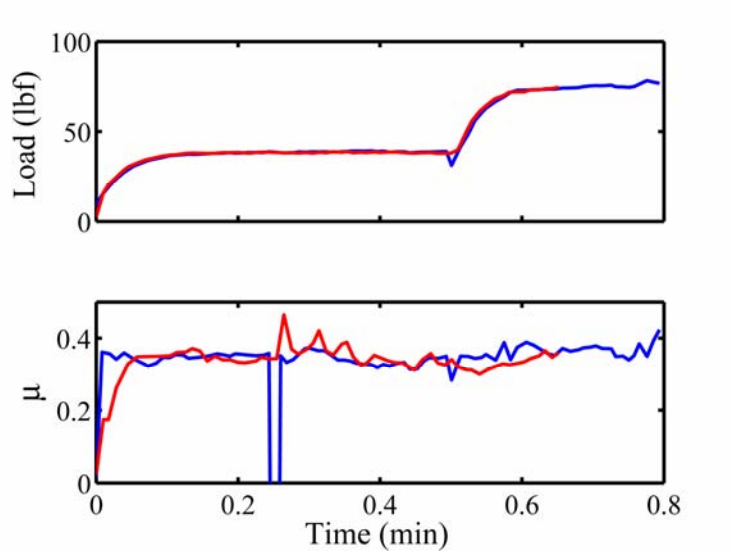

Figure 3.9: Unsuccessful WC/C(B) tests with immediate scuffing

Although, WC/C(B) performed poorly, the same coating with a CrN underlayer produced the lowest steady-state friction coefficient of 0.05 and highest load bearing capacity (455 lbf) of all the coatings. CrN + WC/C(A) was able to achieve the same load, but exhibited a higher steady-state friction coefficient at 0.17 that began to rise for a short period before scuffing. The HPT data for the two types of CrN + WC/C coatings are given in Figures 3.10 and 3.12 as well as representative worn disks and shoes in Figures 3.11 and 3.13. All tests were performed until scuffing failure, but some were stopped before the large increase in friction became apparent. The higher friction generated by CrN + WC/C(A) coating is likely due to the higher initial roughness and the abrasive wear resistance of the hard multi-layer coating, inhibiting running-in. The effects of higher friction were also apparent in the higher temperature attained, exhibited in the discolored shoe in Figure 3.13. It is unknown what causes the friction spikes early in testing with this coating, but they illustrate its tribological consistency.

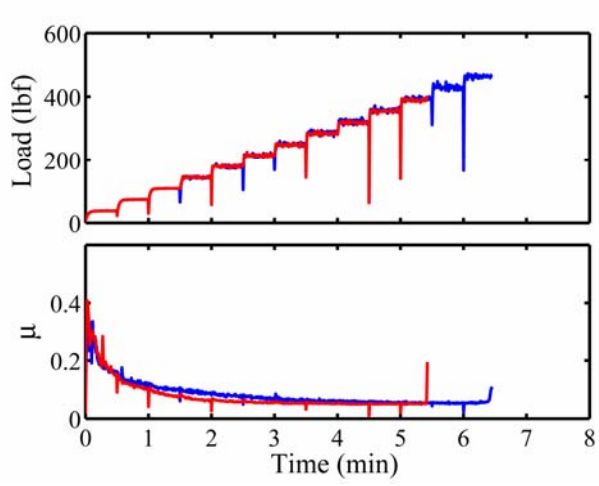

Figure 3.10: HPT data for scuffing of CrN + WC/C(B)

Figure 3.11: Worn CrN + WC/C(B) coated disk and shoe

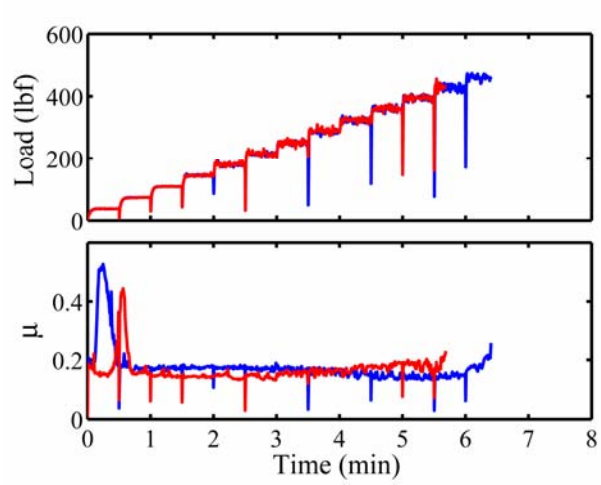

Figure 3.12: HPT data for scuffing of CrN + WC/C(A)

Figure 3.13: Worn CrN + WC/C(A) coated disk and shoe

The CrN underlayer improved the consistency of WC/C + DLC as observed in the HPT data shown in Figures 3.14 and 3.16 with representative worn disks and shoes in Figures 3.15 and 3.17. In this case, however, the CrN increased the surface roughness, similar to WC/C(A), causing a higher friction coefficient. The lowest friction coefficient produced with WC/C + DLC was 0.06 while the CrN underlayer caused the value to increase to 0.11. The increase in friction appeared to increase wear and cause the interface to scuff at a lower load than one, but not both, of the disk without the CrN underlayer.

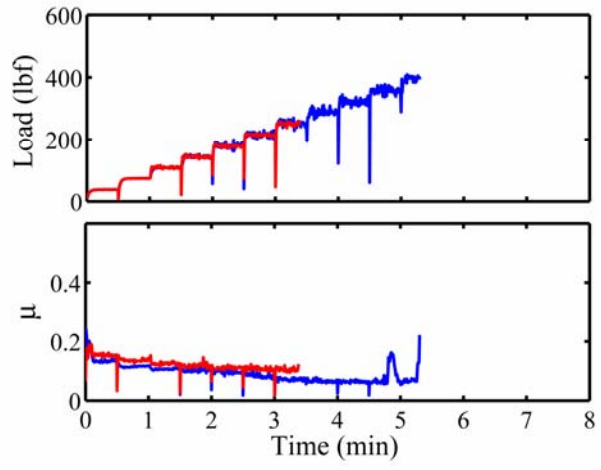

Figure 3.14: HPT data for scuffing of WC/C + DLC

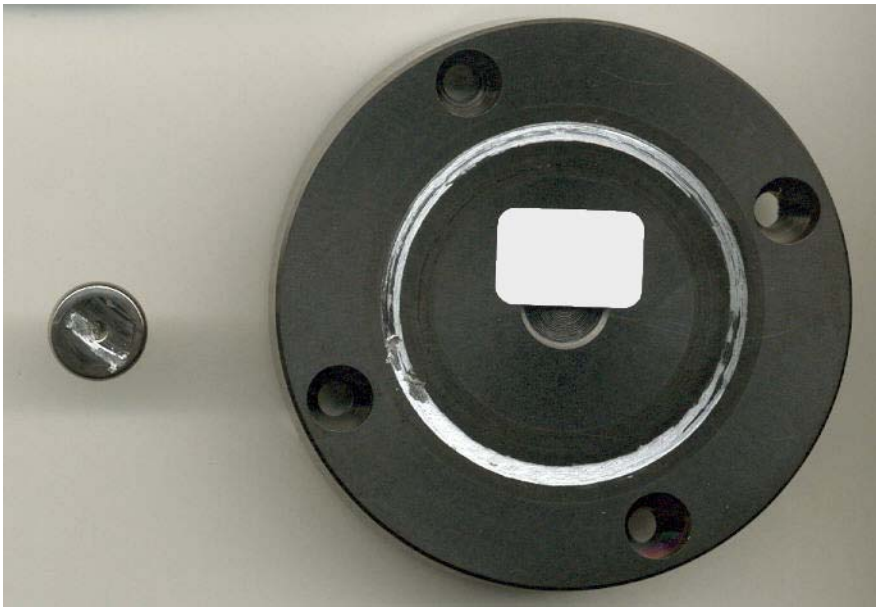

Figure 3.15: Worn WC/C + DLC coated disk and shoe

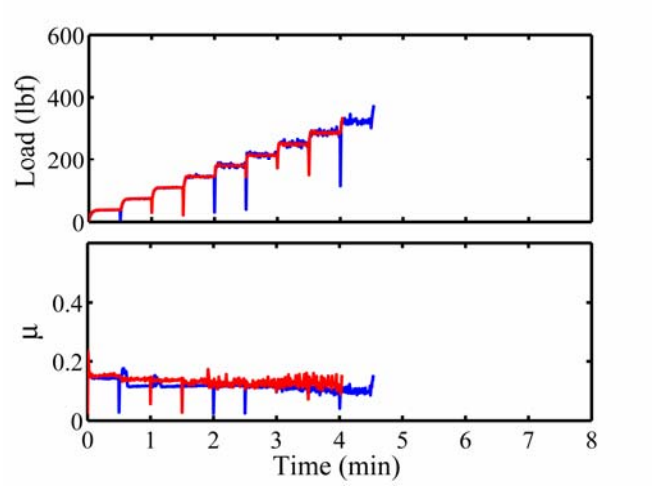

Figure 3.16: HPT data for scuffing of CrN + WC/C + DLC

Figure 3.17: Worn CrN + WC/C + DLC coated disk and shoe

The final test in this series of scuffing experiments was performed with WC/C(A). As the HPT data in Figure 3.18 shows, the scuffing load of 245 lbf (1091 N) is much lower than that of the previous tests due to the load bearing capability of the CrN underlayer. As a result of the lower roughness, though, it produces a friction coefficient of 0.09, about half of that produced with a CrN underlayer, but was still higher than CrN + WC/C(B). The worn disk and shoe are displayed in Figure 3.19.

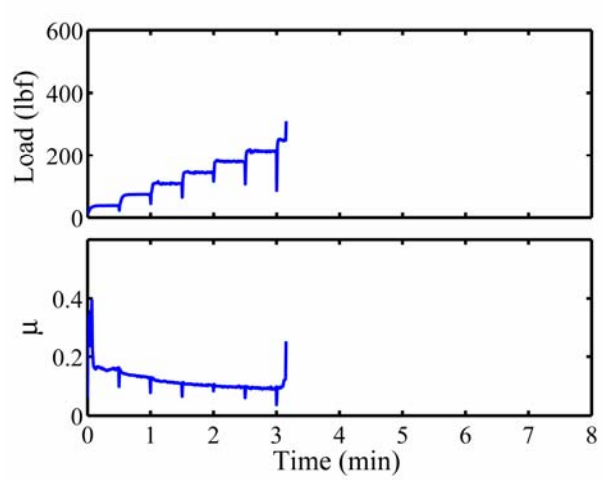

Figure 3.18: HPT data for scuffing of WC/C(A)

Figure 3.19: Worn WC/C(A) coated disk and shoe

Only two successful tests were performed with WC/C(B). To determine if running-in at low loads for an extended period ultimately affected performance, WC/C(B) was tested at 10 lbf (45 N) and 50 lbf (223 N) for 10 minutes each before increasing to 250 lbf (1114 N), as shown in Figure 3.20. Scuffing occurred within a few minutes or less at a similar load to WC/C(A), suggesting similar performance, as expected. However, premature coating failure was never an issue with WC/C(A).

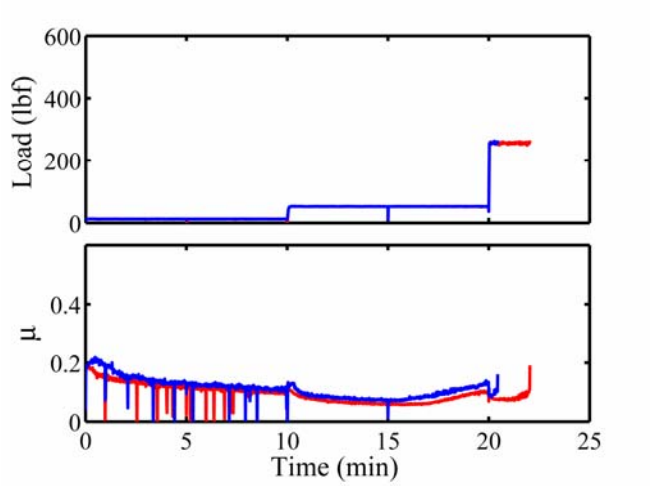

Figure 3.20: HPT data for scuffing of WC/C(B)

A summary of scuffing loads for each coating is presented in Figure 3.21. Based on this testing, the hypothesis that a CrN underlayer improves load bearing capacity is confirmed in the case of WC/C(A) and WC/C(B). However, the deposition of CrN under WC/C(A) increased the overall surface roughness causing significantly increased friction. Still, with a scuffing load over 400 lbf (1782 N), and a friction coefficient of 0.17, the CrN + WC/C(A) coating performs significantly better than uncoated, unlubricated tests. The CrN underlayer improves the quality consistency, ultimately allowing WC/C(B) to achieve the highest load and lowest friction

coefficient of all coatings, but still falls short of fully lubricated tests performed by Demas with scuffing loads of 750 lbf and a friction coefficient of 0.05 [6].

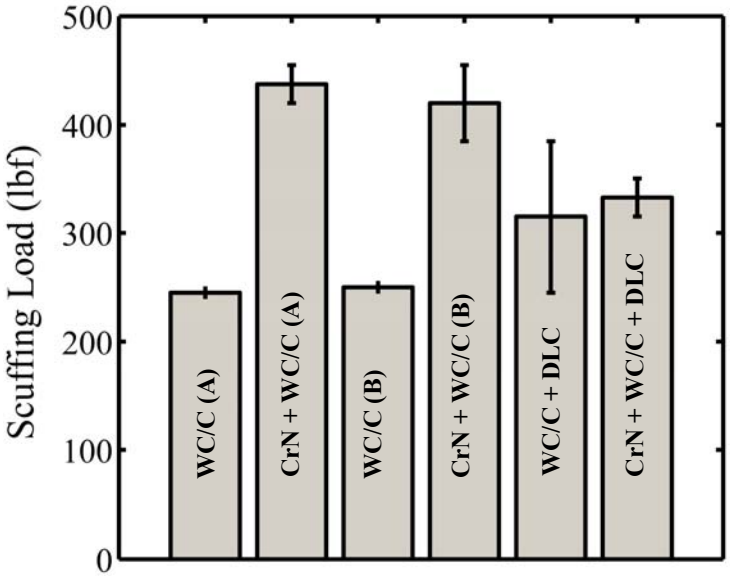

Figure 3.21: Average scuffing loads of tested coatings. Error bars represent the maximum and minimum values for each coating.

3.2 Piston-type compressor Simulation

3.2.1 Preliminary Testing

To obtain a baseline from which to compare coating performance, tests were performed with uncoated pins at room temperature. The aim was to determine at which load the uncoated tests could be run without scuffing failure. Uncoated pins were only able to support a 45 lbf (200 N) normal load for ten minute tests and exhibited a steadily increasing friction coefficient with a final value of 0.32 as shown in Figure 3.22. A running-in period was apparent in the first few minutes where friction reached a maximum and started to decrease. The cause of this running-in period is possibly a result of adhesive wear increasing roughness of both surfaces and subsequently the abrasive wear and friction coefficient as evidenced by material transfer to the pin as well as significant wear debris from the disk. The worn disk and profile scan showing a wear depth of 1-2 μm are displayed in Figures 3.23 and 3.24. Note that scuffed disks had wear depths on the order of 100 μm. No measurable pin wear was observed as mostly material transfer from the disk occurred. In contrast to the behavior exhibited in the uncoated experiments, measurable disk wear was not observed in coated experiments.

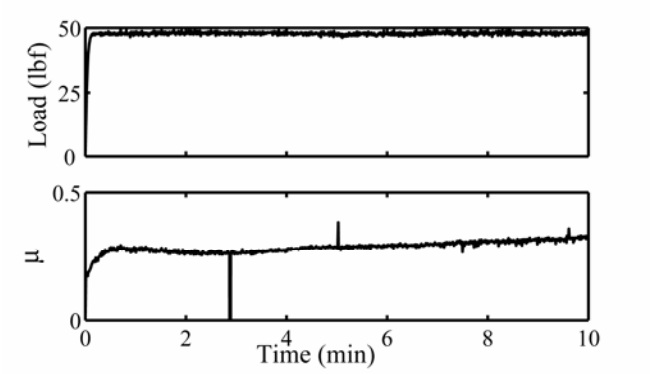

Figure 3.22: HPT data for uncoated test in R134a at 25 psi and 23°C

Figure 3.23: Worn cast iron disk used in uncoated test

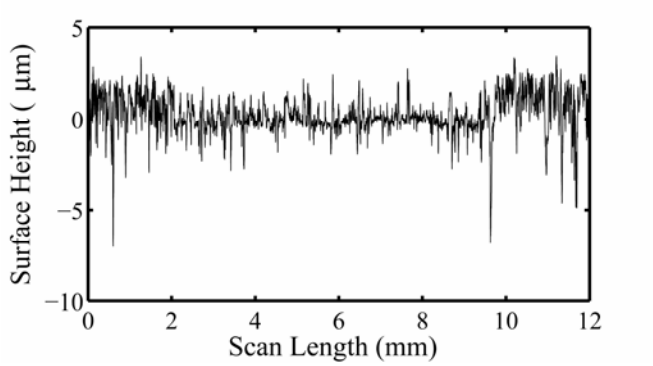

Figure 3.24: Profile scan of worn cast iron disk used in uncoated test

At the opposite extreme, a step-loading test was conducted with WC/C + DLC that was able to withstand 750 lbf (3341 N) before failure. HPT data for this test is shown in Figure 3.25. Note that the long step duration in the middle of the test was a result of two tests run back to back using the same specimens. The original maximum load was set of 500 lbf (2227 N) which did not result in scuffing, so the load was set higher and the test restarted with the specimens still in contact under load. This is a remarkable feat considering the uncoated results and the presence of very little wear debris due to mostly plastic deformation as evidenced by the leftover machining marks in Figure 3.26. Also interesting to note is that the coating was not worn through, but failure was caused by extreme plastic deformation of the disk as depicted by the disk wear scan in Figure 3.27. The radius of the worn pin determined from the pin wear scan in Figure 3.28 was ~4.6 mm indicating a final Hertzian contact pressure of 1.6

GPa. A contact pressure of this magnitude could not be accomplished with other coatings, and therefore, this test was not repeated.

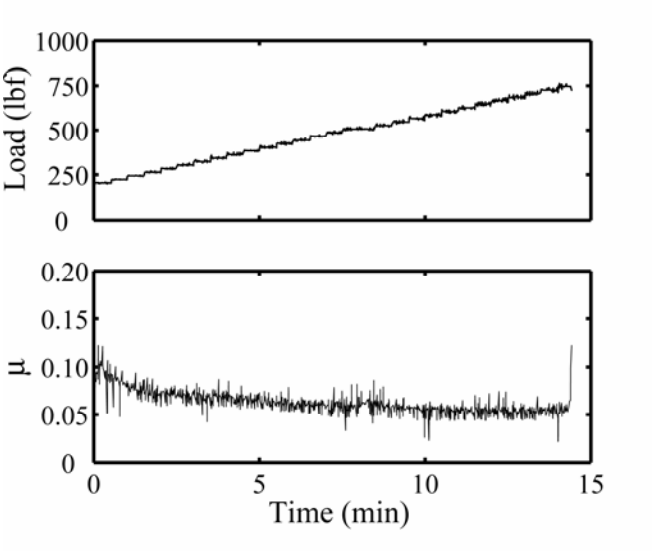

Figure 3.25: HPT data for step-loading test with WC/C + DLC in R134a at 25 psi and 23°C

Figure 3.26: Image of worn cast iron disk showing plastic deformation in step-loading test

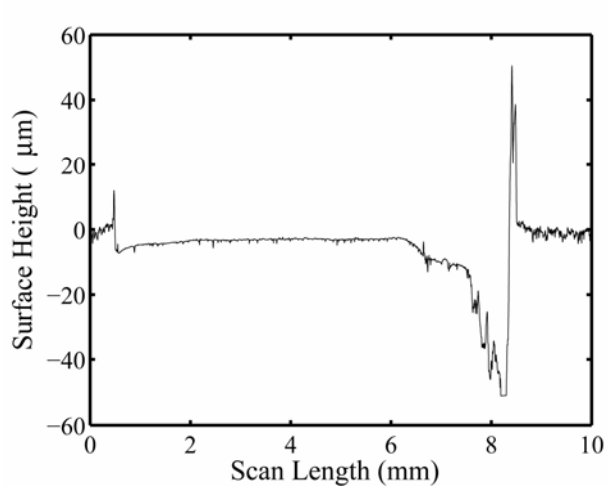

Figure 3.27: Disk wear scan performed perpendicular to sliding direction

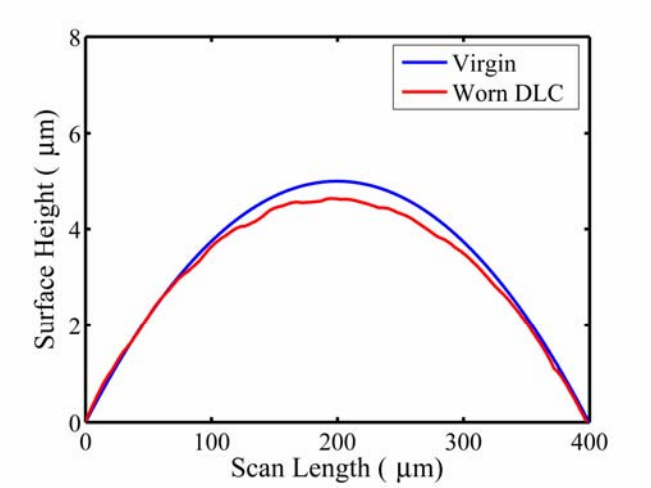

Figure 3.28: Pin wear scan performed parallel to sliding direction

Constant load experiments were also conducted with the WC/C + DLC coating. Figure 3.29 shows images of the disks with their respective loads and friction coefficients. Again, the wear was mostly plastic deformation with a depth of less that 1 µm on the disk for 300 lbf, as depicted in Figure 3.30. Similar to the step-loading tests, the friction coefficient appeared to decrease with increasing load. While it is certainly interesting that the interfaces are able to sustain these loads, lower constant loads with longer durations must be used for comparison to coatings with lower load bearing capability.

Similar to the shoe-on-disk testing, the TiAlN + WC/C coating was deemed unsuitable for the pin-on-disk testing. The coating produced higher friction than that of the uncoated experiment at a load of only 50 lbf (223 N) and was eliminated from further testing. A possible cause of this, as indicated by cross-sectional SEM in Figure 3.5, is that the WC/C overcoat is relatively thin compared to other coatings, and is quickly worn off, exposing the high friction TiAlN underlayer.

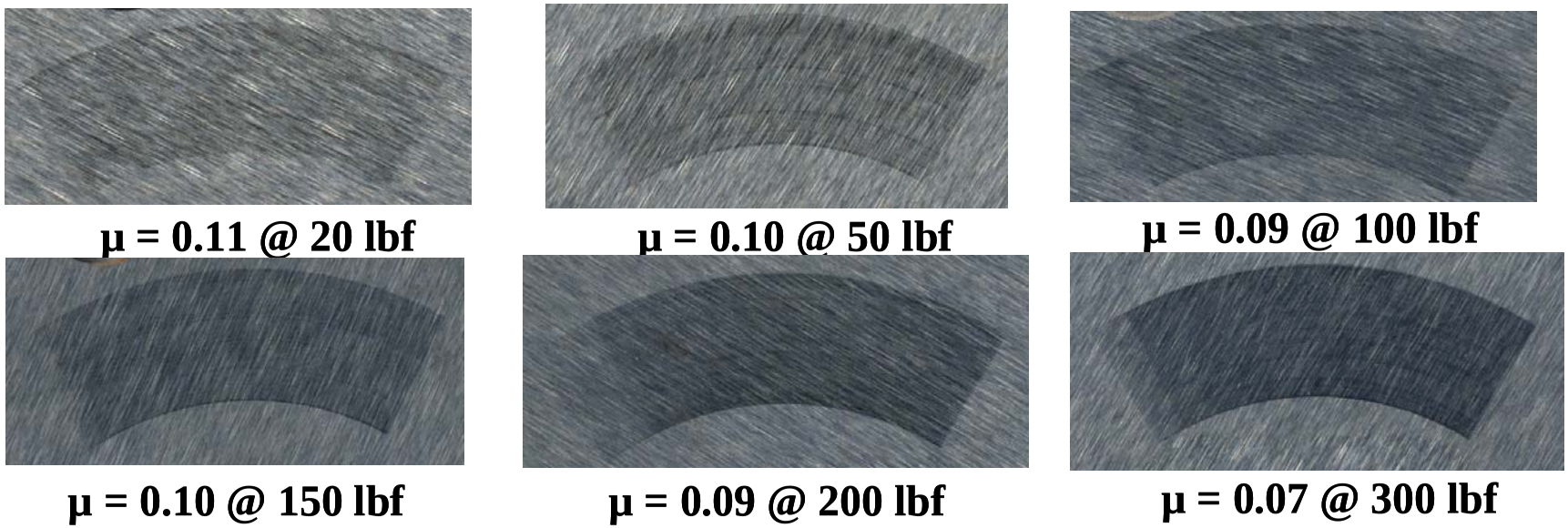

Figure 3.29: Images of worn cast iron disks in constant load preliminary tests

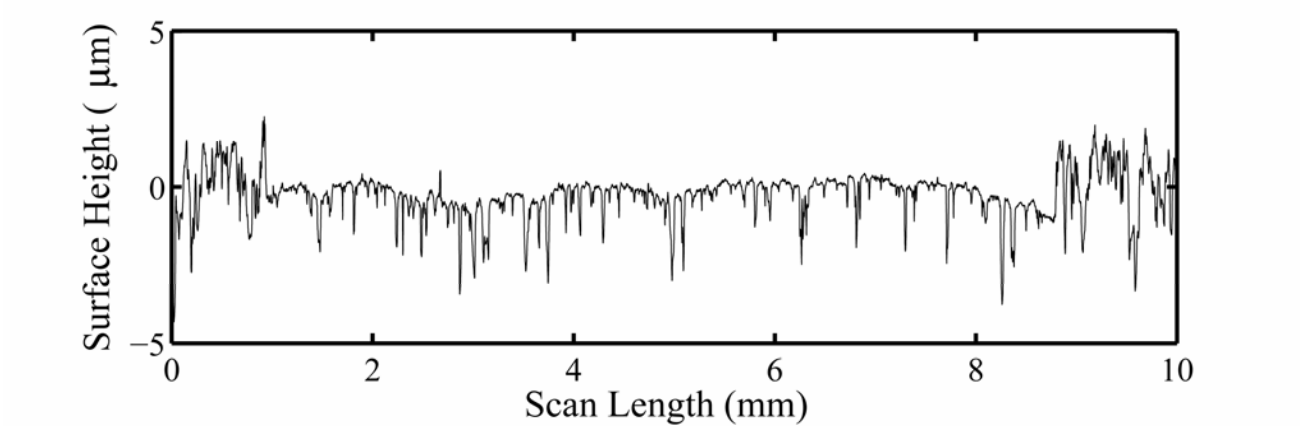

Figure 3.30: Profile scan of worn disk after 300 lbf test

3.2.2 Temperature Variation

Due to insignificant disk wear produced in coated experiments (depths < 0.5 µm, indistinguishable from the disk roughness) while pin wear became significant, only pin wear was quantified. Steady-state friction coefficient values and wear rates, defined as wear volume per total sliding distance, for coated and uncoated pins are depicted in Figures 3.31 where error bars represent the minimum and maximum values for a given condition. As the error bars indicate, test repeatability was high. Steady-state friction coefficients are shown to decrease with temperature while wear rates initially decreased and then increased at the highest temperature tested. At temperatures below 60°C, WC/C + DLC performed slightly better in terms of friction than the other coatings with a value of 0.12, but the trend was reversed at 60°C with WC/C from both manufacturers performing similarly and WC/C(A) showing the lowest friction coefficient of 0.05 at 120°C (normal load of 50 lbf). This is possibly due to WC/C's ability to form a more effective transfer layer than pure DLC in some conditions [1]. However, the pin wear of WC/C + DLC is significantly better than the others with less than one third of the wear at 60°C and about 40% less at 120°C. This is undoubtedly a result of the DLC overcoat's higher hardness. In fact, the DLC overcoat is never worn through as depicted in Figure 3.32 where the green line denoted the boundary below which the WC/C underlayer starts, and the black line is the boundary below which the 52100 steel substrate starts.

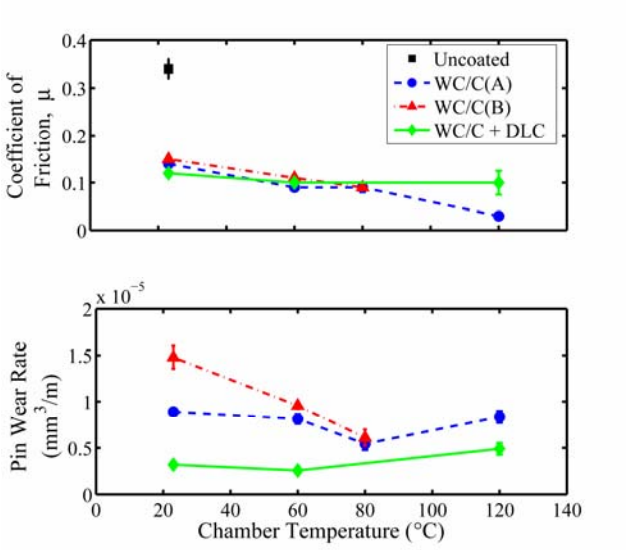

Figure 3.31: (a) Steady state coefficient of friction and (b) pin wear rate versus temperature for uncoated and coated pins. Note that WC/C(A) at 120°C was tested at 50 lbf. Error bars represent maximum and minimum values for a particular condition.

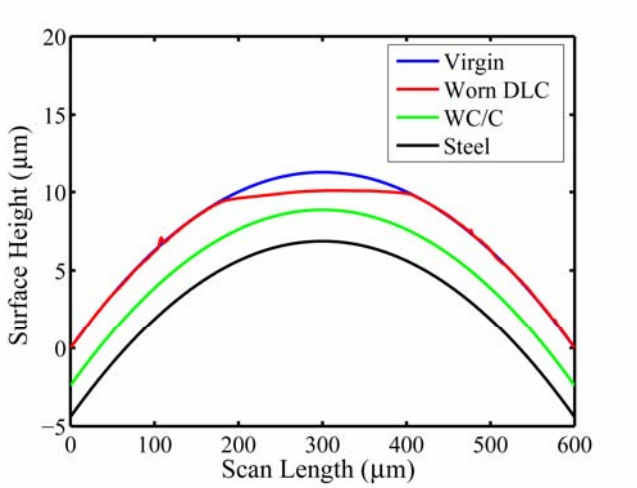

Figure 3.32: Pin wear scan of WC/C + DLC at 120°C. The green line denotes the boundary below which the WC/C underlayer starts, and the black line is the boundary below which the 52100 steel substrate starts.

At room temperature, no significant running-in period was observed, reaching steady-state almost immediately after the 50 lbf wear-in load. This is likely due to low adhesive wear from the low surface energy of the coating while the disk surface was quickly polished. At temperatures of 60°C and above, however, adhesive wear began to increase, increasing the pin wear rate. As wear of the pin increased with temperature, it is postulated that a transfer film on the disk from the coating begins to form causing the steady-state friction coefficient to decrease, which is in agreement with the literature [9-12, 17]. Also contributing to the friction decrease was a higher polishing rate of the disk surface at increased temperatures. It is important to note, however, that disk wear was still not measurable while pin wear rates decreased in the transition from room temperature to 60°C, with WC/C(B) exhibiting the largest decrease. Wear rates decreased further from 60°C to 80°C for both WC/C coatings, but steady-state friction coefficients remained similar with initial running-in values of 0.2-0.25. Increased wear and similar friction is due to a transition period from abrasive to adhesive wear in this temperature range. An increase in temperature to 120°C produced a lower steady-state friction coefficient for WC/C(A) while the transition to adhesive wear increases the pin wear rate by over 50% from values at 80°C. The increase in adhesive wear was evidenced by greater material flow on the coating surface at higher temperatures, as observed with SEM, which also caused pronounced running-in periods.

3.2.3 Running-in at Elevated Temperatures with WC/C(A)

During tests conducted at 120°C, a very pronounced running-in period was observed with friction coefficients reaching in excess of 0.4, but would then attain steady-state values of less than 0.05. To study this running-in behavior, additional tests were performed that were stopped at the friction coefficient peak (5 minutes) and at the end of the running-in period (10 minutes). Tests were repeatable and plots are shown with load and friction evolution in Figure 3.33, exhibiting the same trend of high values in running-in and attaining steady-state thereafter. Notice also in Figure 3.34 that friction immediately reaches steady-state at 23°C, while running-in friction coefficients increased with temperature. While running-in is investigated for only WC/C(A), the same

trends are apparent for all coatings. It is possible that the cause is something common to all coatings, such as similar roughness.

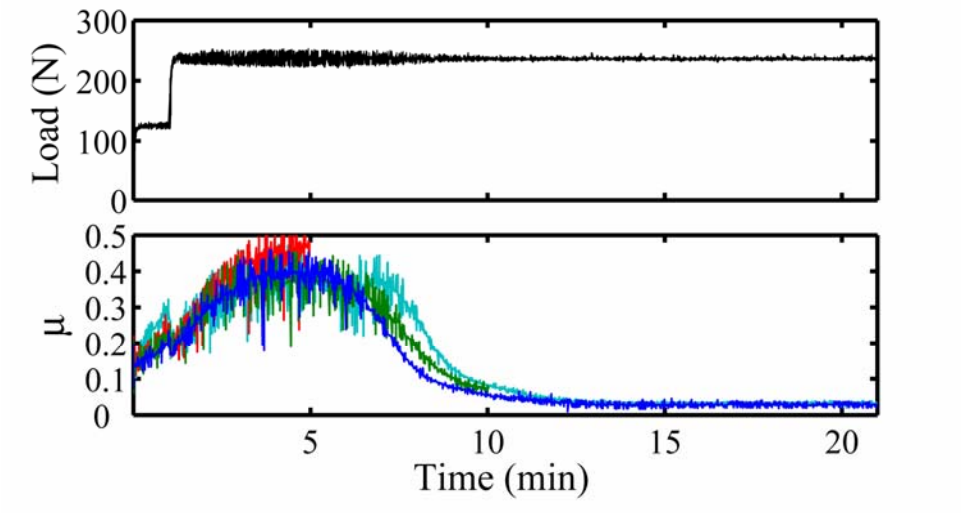

Figure 3.33: Load and friction coefficient, μ, evolution for WC/C(A) with test durations of 5, 10, and 21 minutes (full length). Note the test repeatability and apparent noise caused by oscillatory motion.

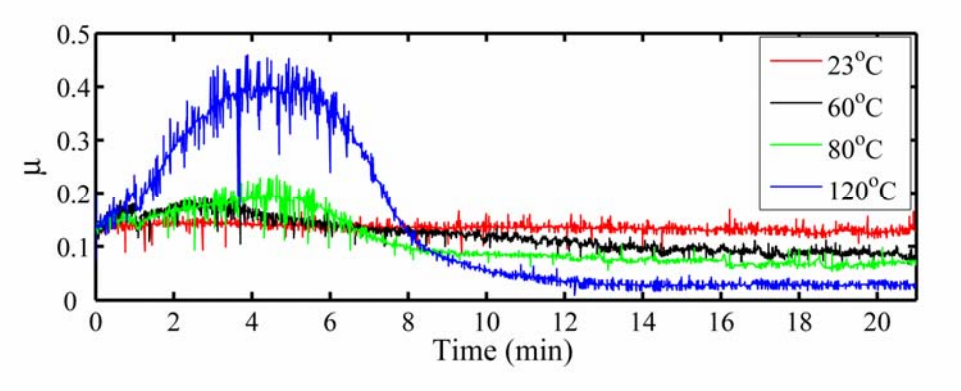

Figure 3.34: A comparison running-in characteristics in terms of the friction coefficient of WC/C (A) for each temperature tested.

As postulated, nearly all pin wear occurred during the running-in period with little or none during steady state. The pin wear volume for the 5, 10 and 21 minute tests were 1.68 x 10^{-3} mm^3, 2.44 x 10^{-3} mm^3, and 2.37 x 10^{-3} mm^3, respectively. Although, the volume at 10 minutes was measured to be more than 21 minutes, the values are within 3% and are essentially equal. The pin wear volume at 5 minutes, suggests that the majority of the wear occurs during the first half of the running-in period. Illustrating material transfer to and from the disk, SEM images of the entire wear tracks and close-ups of the wear track edges are displayed in Figures 3.35 and 3.36. The image taken after the 5 minute test shows that only polishing of the pin occurred with possibly some material transfer from the coating to the disk. However, the images taken after the 10 and 21 minute tests show possible coating material flow or material transfer from the disk.

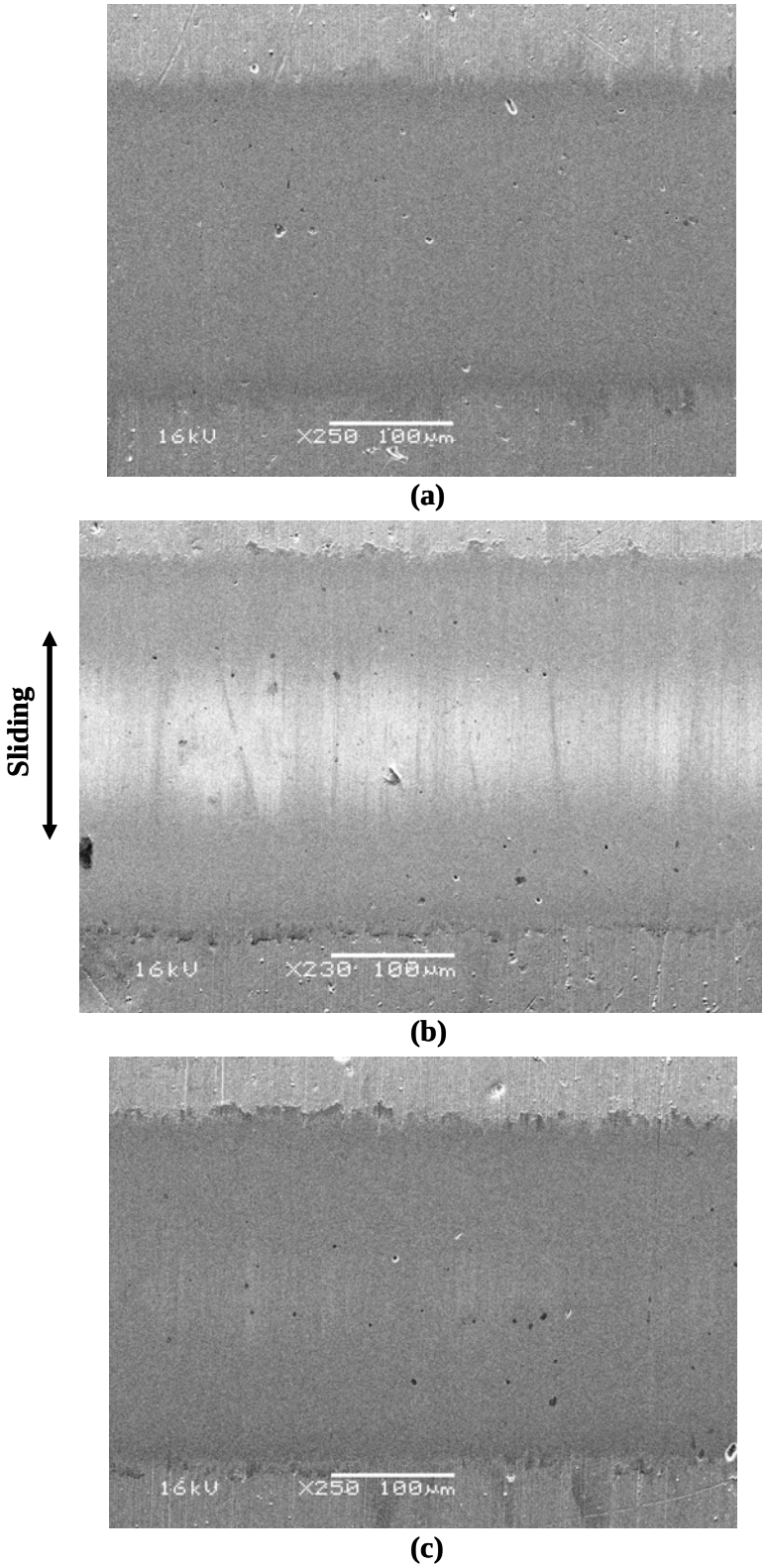

Figure 3.35: Surface SEM images of pin wear after (a) 5, (b) 10, and (c) 21 minute tests at 120°C. Image (b) was taken at X230 and magnified to match the scales of (a) and (c).

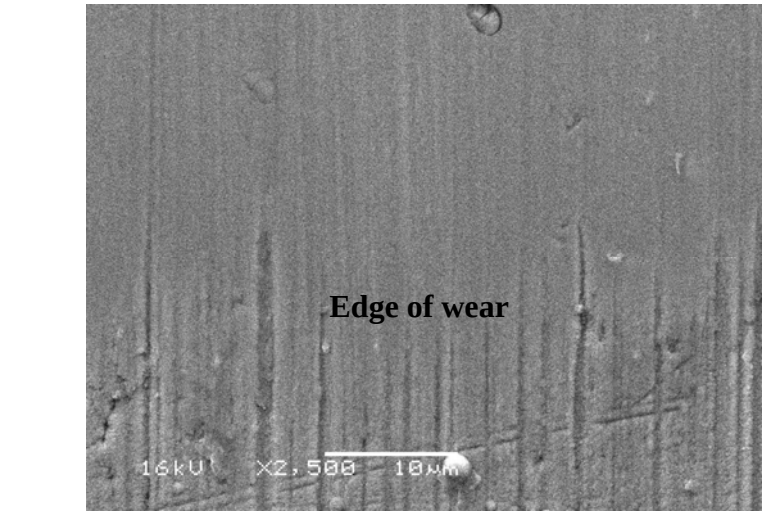

(a)

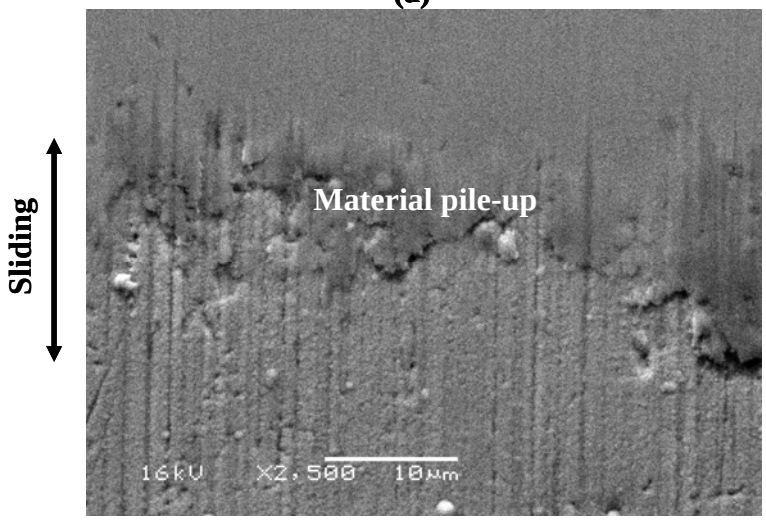

Sliding

(b)

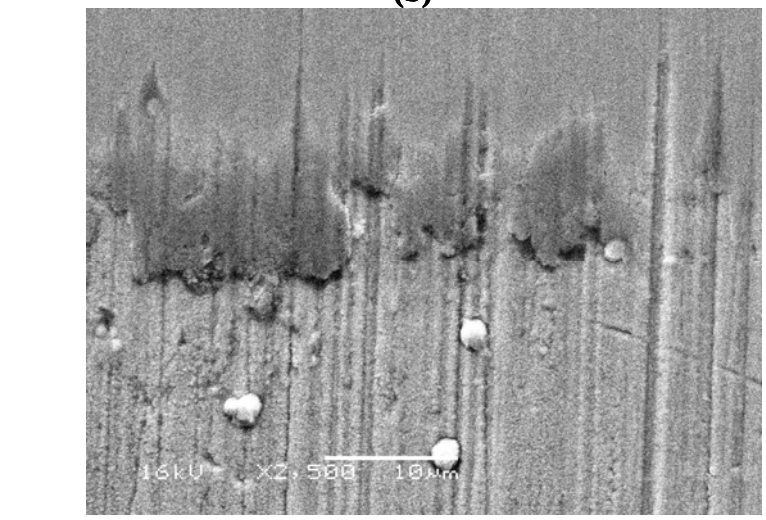

(c)

Figure 3.36: X2500 Surface SEM images of the edge of pin wear after (a) 5, (b) 10, and (c) 21 minute tests at 120°C.

As mentioned previously, it was postulated that a transfer film from the coating to the disk occured, which may have caused a decrease in friction. Such a transfer film would likely be more apparent at higher temperatures due to increased adhesion, causing the pronounced running-in period. The evidence of transfer films was investigated using EDS on a JEOL 6060LV SEM for WC/C(A) at 120°C. To provide an explanation for running-in, a thicker transfer film should be apparent for the 10 and 21 minute tests versus the 5 minute tests. However, the wt. % of tungsten (the only defining element of WC/C(A) since cast iron contains carbon) ranged from 1 to 3% with no correlation to the test times. This suggests that the transfer film forms early on and is most likely not the cause of the running-in period. Representative EDS spectra for 5 and 10 minute tests are shown in Figures 3.37 and 3.38 with the corresponding compositions in Table 3.2. Note that the tungsten composition at 10 minutes is less than at 5 minutes. Some spectra at 10 minutes showed greater tungsten composition than at 5 minutes, though, rendering these results inconclusive as a single explanation for the running-in period.

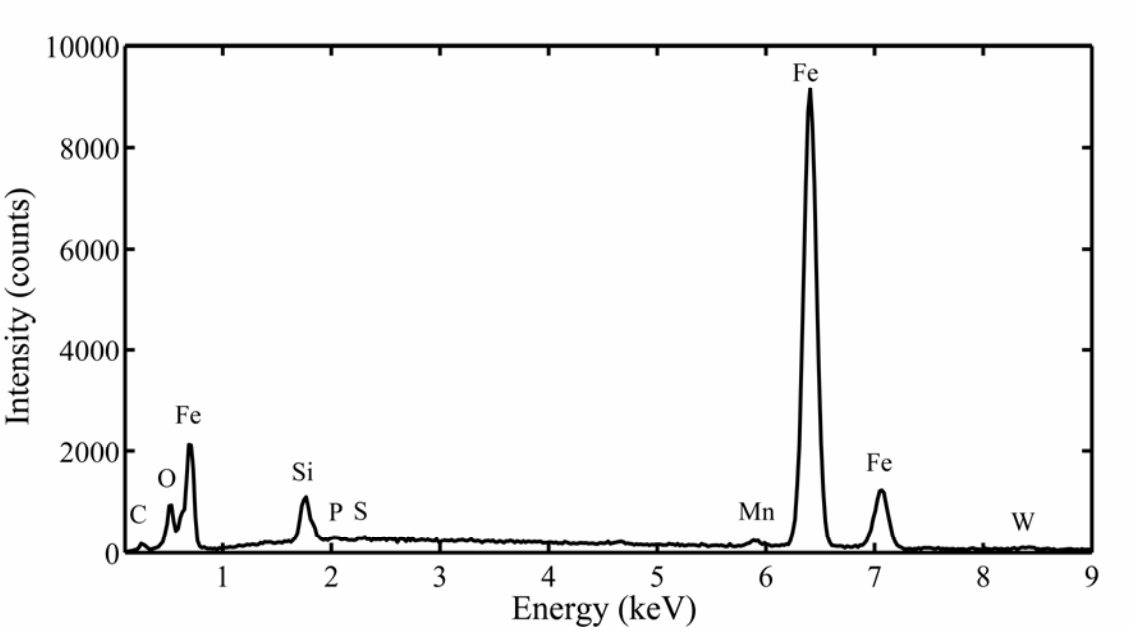

Figure 3.37: EDS spectrum of worn cast iron disk after 5 minute test

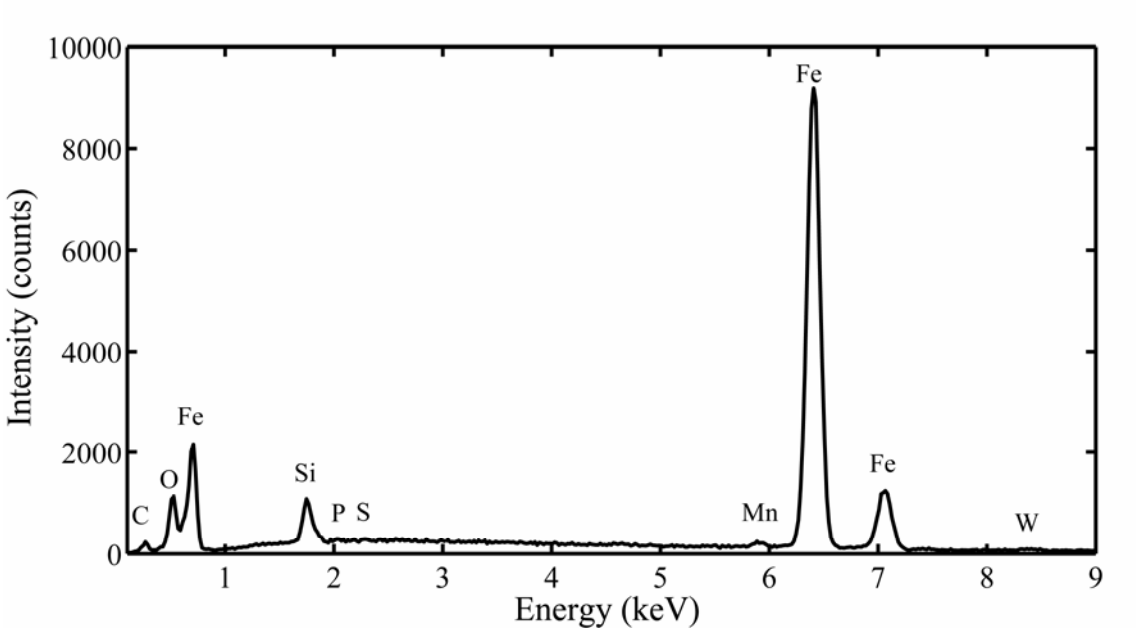

Figure 3.38: EDS spectrum of worn cast iron disk after 10 minute test

Table 3.2: Elemental composition of bulk cast iron, virgin surface, and worn surface

	Element (wt. %)											
	C	**Cr**	**Cu**	**Fe**	**Mn**	**O**	**P**	**S**	**Sb**	**Si**	**Sn**	**W**
Mfr. Spec.	2.7-4	>0.05	0.05-0.30	95	0.60-0.95	-	0.05-0.20	0.03-0.07	0.02-0.2	1.8-3.0	0.1-0.3	-
Virgin EDS	3.36	-	-	93.72	0.89	-	0.16	-	-	1.88	-	-
EDS: 5min.	2.91	-	-	86.61	0.86	4.76	0.14	0.09	-	1.69	-	2.95
EDS: 10min.	3.44	-	-	86.06	0.69	5.95	0.07	0.04	-	1.78	-	1.97

To further examine running-in, profilometric scans of the pins and disks were performed perpendicular to the sliding direction within the central 4 mm of the wear scar. Figures 3.39 and 3.40 depict profiles of worn and corresponding virgin pins and disks, and relative roughness and skewness values are listed in Table 3.3. A difference is clearly seen in that during the first 5 minutes, pin micro-roughness significantly decreased through the shearing of asperity peaks. From 5 to 10 minutes, the roughness increased, likely due to the conforming wear caused by the rougher disk. At 21 minutes, overall pin roughness decreased due to polishing while microroughness increased slightly, as it did on the disk.

Although the virgin roughnesses of the two virgin disks were quite different (Rq = 517 nm vs. Rq = 299 nm), it is important to note that the roughness always decreased with test time. More interesting, however, is that the negative skewness was greater for longer tests due to increased polishing. It is possible that the polishing process was the cause of the running-in period. At low temperatures, the polishing process may have been accelerated, causing a less severe and shorter running-in period.

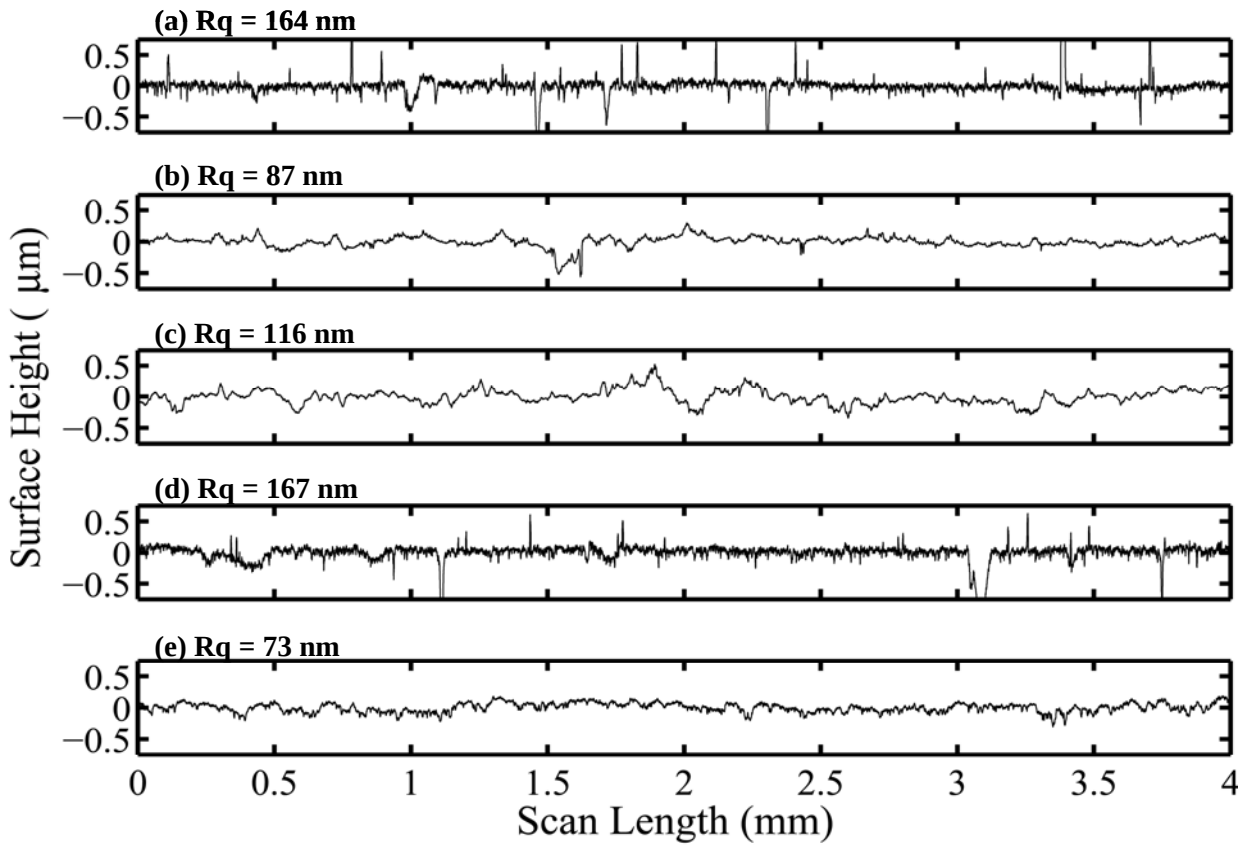

Figure 3.39: Representative profile scans of (a) a virgin pin used for 5 and 10 minute tests, (b) pin roughness after 5 minutes, (c) pin roughness after 10 minutes, (d) virgin pin used for 21 minute test, and (e) pin roughness after 21 minutes. Scans were performed perpendicular to the sliding direction.

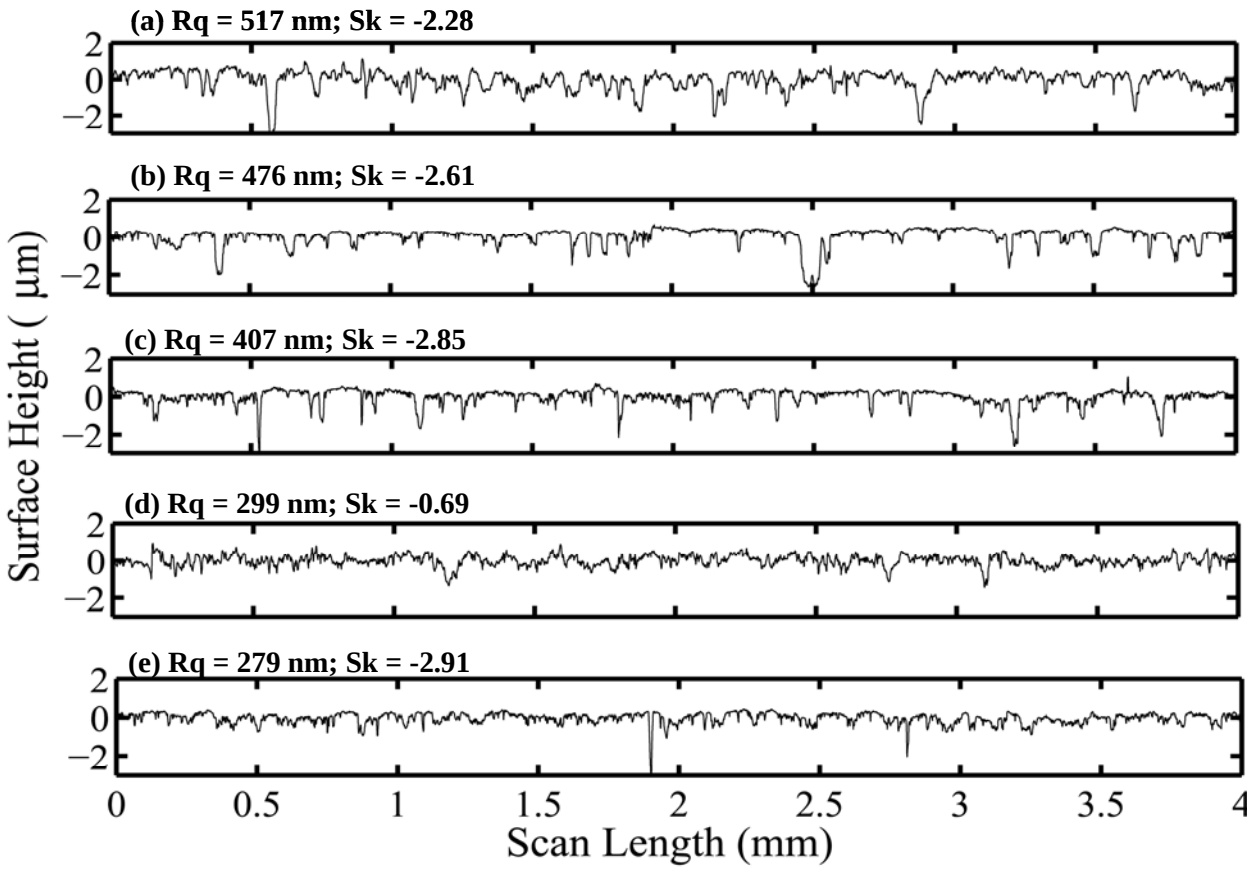

Figure 3.40: Representative profile scans of (a) a virgin disk used for 5 and 10 minute tests, (b) disk roughness after 5 minutes, (c) disk roughness after 10 minutes, (d) virgin disk used for 21 minute test, and (e) disk roughness after 21 minutes. Scans were performed perpendicular to the sliding direction.

Table 3.3: Roughness and skewness of specimens used for running-in investigation

	Pin	Disk	
Test	**Rq (nm)**	**Rq (nm)**	**Sk**
Virgin (5 & 10 min. tests)	164	517	-2.28
5 minutes	87	476	-2.61
10 minutes	116	407	-2.85
Virgin (21 min. test)	167	299	-0.69
21 minutes	73	279	-2.93

Relative roughness can also be clearly seen in SEM images of disk surfaces at magnifications of X500 and X2500 in Figure 3.41. The images confirm that material flow of the cast iron occurred, progressively filling in valleys with material that was removed from asperity peaks, increasing negative skewness and decreaseing roughness. The roughness and skewness values along with the evolution of the pin and disk wear profiles demonstrate that pin and disk surfaces conformed to each other through polishing and material transfered to reduce abrasive friction and complete the running-in process. For real engineering applications, it would be best to polish

contacting surfaces before coating. As this can be costly or unfeasible, proper running-in procedures should be investigated to optimize tribological performance.

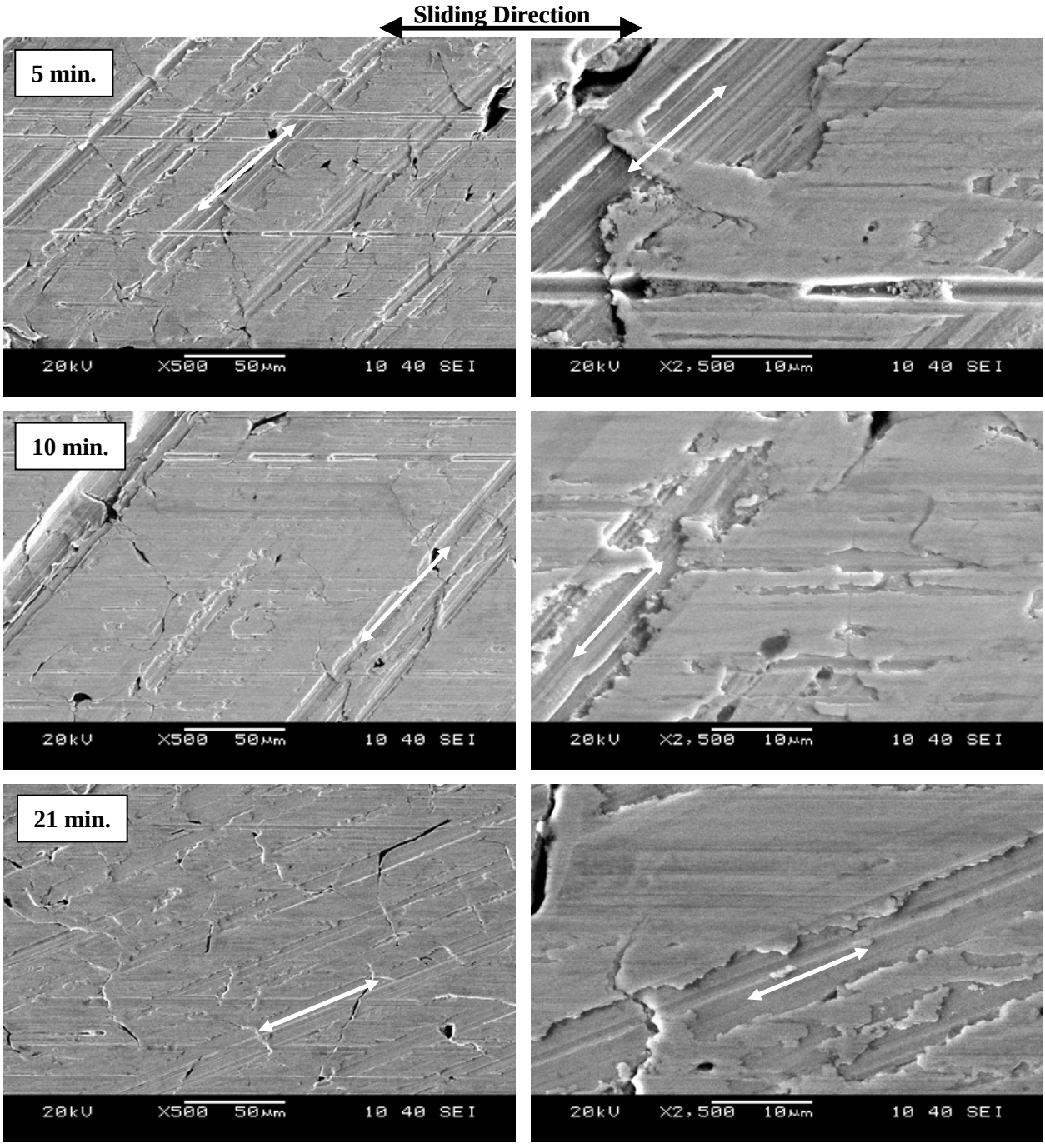

Figure 3.41: X500 (left column) and X2500 (right column) SEM images of cast iron disks from WC/C(A) tests at 120°C and various durations. White arrows on images denote machining mark directions.

3.2.4 Refrigerant Variation

Due to the absence of literature on refrigerant comparison, it was unsure how each refrigerant would perform relative to each other. HPT friction and load data are shown for representative experiments for each

environment in Figure 3.42. It was found that friction coefficients for R134a, R410a, and N_2 were similar in the first few minutes with the WC/C + DLC coating, but then scuffing occurred in the N_2 environment at a little over four minutes. This is not surprising as interfaces tend to have less wear in refrigerant environments versus air [7]. At around five minutes, the R410a interface exhibited decreasing friction indicating that it was in a state of running-in. It reached steady-state with slightly lower friction than in the R134a environment, but the friction in the R600a environments remained the lowest for the entire test. Steady-state friction coefficients for each environment are displayed in Figure 3.43. Note that the friction coefficient for N_2 was the average prior to scuffing. Chemical analyses were not performed to detect compounds that may improve friction or wear characteristics, but R600a has the highest percentage of hydrogen atoms per unit volume (Table 3.4), and Fontaine et al. found that H_2 has a healing effect on hydrogenated DLC coatings in tribological applications enabling lower friction but not necessarily wear [22]. Conversely, R410a produced the least amount of wear with R600a being the second best. Reasons for this are unknown without further chemical analyses. Relative pin wear rates are given in Figure 3.44. Also, note that wear is not reported for N_2 due to extreme material transfer with scuffing failure.

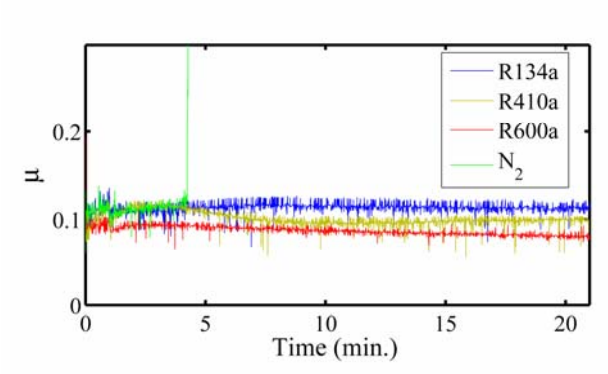

Figure 3.42: Representative friction coefficient evolution for various environments

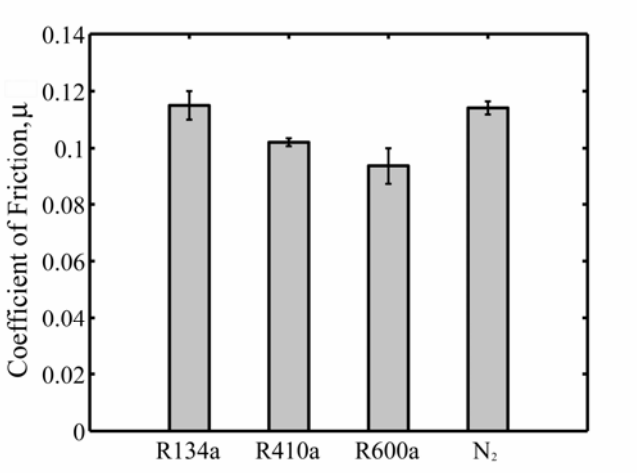

Figure 3.43: Friction coefficients for the WC/C + DLC coating in various refrigerants. Error bars represent maximum and minimum values for a particular condition.

Table 3.4: Element composition by % vol. for various refrigerants

Refrigerant	Molecular formula	Element		
		C	H	F
R134a	$F_3C\text{-}CH_2F$	27.4	13.9	38.5
R410a	$CH_2F_2 + F_3C\text{-}CHF_2$	54.8	69.5	0.0
R600a	$(CH_3)_2CH\text{-}CH_3$	17.8	16.6	61.5

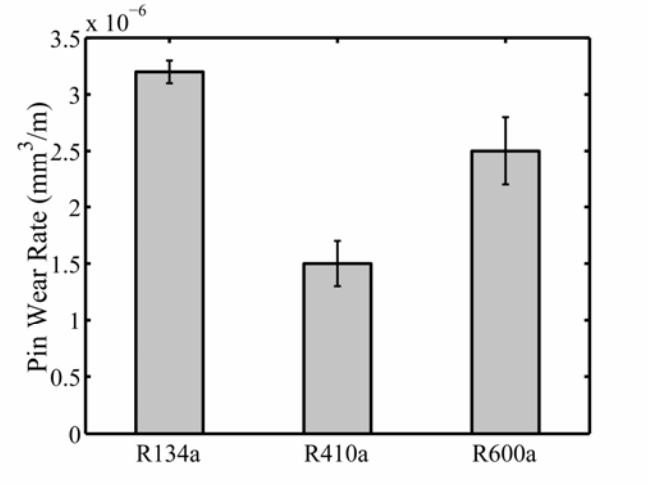

Figure 3.44: Pin wear rates for various environments. Note that N_2 is not shown due to severe damage caused during scuffing.

3.2.5 Frequency Variation

Limited testing was conducted to study how speed affected friction and wear. In general, increased velocity appeared to cause higher wear, as shown in Figure 3.45 with the exception of WC/C(A). However, the decrease is too small to conclude that wear is proportional to speed. Also, the friction coefficient for all three coatings increased slightly with increasing velocity. Only two frequencies were tested, though, producing limited data on the affects of velocity. It was decided that frequencies lower than 4.5 Hz (0.21 m/s) were not relevant to piston-type compressors and this group of testing was discontinued due to the limitations of the HPT.

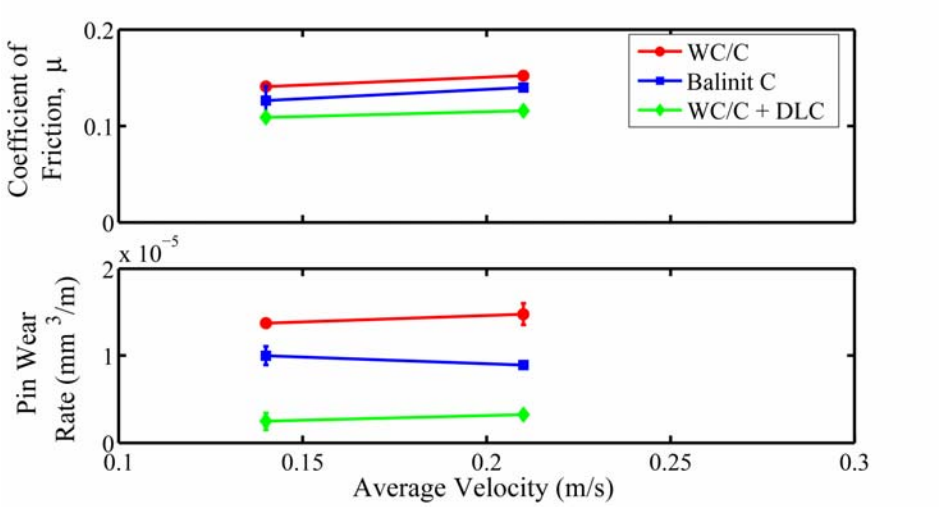

Figure 3.45: Coefficient of friction and pin wear rate dependence on velocity

Chapter 4: Conclusions and Recommendations

4.1 Swashplate Compressor Simulation

The application of hard coatings to the A390-T6 surface greatly improved the tribological performance of the swashplate compressor simulation. Without coatings or lubrication, the shoe-on-disk interface was hardly able to support 15 lbf while producing a very unstable friction coefficient. However, thought step-loading experiments, the best performing coating, CrN + WC/C(B), was able to support loads as high as about 450 lbf with a friction coefficient of ~0.5.

It was difficult to investigate wear with this interface as the cause of scuffing was due to poor load support by the soft aluminum substrate rather than wearing through the coating. Mostly step-loading experiments were conducted because of this and the coatings were judged by their maximum scuffing load and friction coefficient. TiAlN + WC/C was eliminated early in testing due to immediate scuffing, possibly caused by poor coating adhesion or relatively thin low friction WC/C overcoat, quickly uncovering the high friction TiAlN underlayer. The lowest performing coating after TiAlN + WC/C was WC/C(B) with a scuffing load of 250 lbf. While this is the same scuffing load as WC/C(A), WC/C(B) performed very inconsistently due to scuff marks that were produced during shipping of the coated disks, even though both types of coatings were shipped in the same manner. WC/C + DLC was able to support a maximum load of just over 300 lbf, although the friction coefficient was slightly larger than the single-layer WC/C. Consistency was a problem with WC/C + DLC as well, but the CrN underlayer improved this, increasing the load support to ~325 lbf.

The best performing coatings were both CrN + WC/C. Both were able to support ~450 lbf in some cases, but the WC/C(A) overcoat caused higher friction due to greater roughness. CrN + WC/C(A) was slightly more consistent, but CrN + WC/C(B) had a lower friction coefficient of 0.05, about half that of CrN + WC/C(A).

4.2 Piston-type Compressor Simulation

The application of hard coatings to 52100 steel pins greatly improved the tribological performance of the piston-type compressor simulation as well. Without coatings or lubrication, the pin-on-disk interface would only support 45 lbf before scuffing occurred. These tests produced friction coefficients of ~0.3 and a disk wear depth of about 1 μm. In contrast, most experiments with coated pins produced negligible disk wear, and the WC/C + DLC coating was able to support 750 lbf with a minimum friction coefficient of 0.06 before failure due to plastic deformation of the disk in a step-loading experiment.

In constant load experiments, the coatings used in this research enhanced tribological performance greatly by reducing the friction coefficient by factors of 3.5 and almost ten for WC/C and WC/C + DLC, respectively, at high temperatures and virtually eliminating wear of the uncoated disk. WC/C + DLC consistently showed the least wear while friction for WC/C(A) and WC/C(B) are slightly higher at lower temperatures, a trend that is reversed at elevated temperatures. The friction coefficients decreased with temperature while wear decreased and then increased following a critical point in temperature where running-in wear becomes more severe. Following running-in, minimal additional wear occurs, indicating the advantage of using coatings with good running-in characteristics and reducing the initial roughness of the interface as much as possible. The cause of running-in is believed to be roughness as the pin and disk conform to each other more throughout the test.

In the refrigerant investigation, experiments in R410a produce the least amount of wear, about half that of R134a. However, tests in R600a exhibited the lowest friction coefficient of about 0.09 possibly due to the abundance of hydrogen in the environment. Tests in R134a, produced the highest friction at almost 0.12, similar to N_2. It was found that refrigerant increases tribological performance as the inert N_2 environment produced scuffing failure.

4.3 Recommendations for Future Testing

While it has already been shown the hard coatings greatly improve the tribological characteristics of compressor surfaces, it is believed that other test parameters and coatings that were not able to be studied here may further enhance performance. Recommendations include:

- Investigate substrate roughness effects
- Test polymer based coatings such as ATSP from the University of Illinois and coatings from other manufacturers such as General Magnaplate for use on soft substrates
- Investigate wear mechanisms and transfer films further with more in depth chemical analyses
- Test in more environmentally friendly refrigerants such as CO_2 at high pressures
- Investigate Si-based and other coatings with greater adhesion characteristics
- Investigate non-hydrogenated DLC coatings that may perform differently with oil under starved lubrication conditions.

References

1. Sung, H.C., "Tribological characteristics of various surface coatings for rotary compressor vane," 221 (1998) 77-85.
2. Lee, Y.Z., Oh, S.D., "Friction and wear of the rotary compressor vane-roller surfaces for several sliding conditions," Wear 255 (2003) 1168-1173.
3. Pergande, S.R., Polycarpou, A.A., "Nanomechanical Properties of Aluminum 390-T6 Rough Surfaces Undergoing Tribological Testing," Journal of Tribology, 126 (2004) 573-582.
4. Yoon, H.K., "Scuffing Under Starved Lubrication Conditions," Ph.D. Thesis, University of Illinois at Urbana-Champaign, 1999.
5. Patel, J. J., "Investigation of the Scuffing Mechanism Under Starved Lubrication Conditions Using Macro, Meso, Micro and Nano Analytical Techniques," M.S. Thesis, University of Illinois at Urbana-Champaign, 2001.
6. Demas, N., "Tribological Studies on Scuffing Due to the Influence of Carbon Dioxide Used as a Refrigerant in Compressors," M.S. Thesis, University of Illinois at Urbana-Champaign, 2003.
7. Cannaday, M., "Tribology of Unfilled and Filled Polymeric Surfaces in Refrigerant Environment for Compressor Applications," M.S. Thesis, University of Illinois at Urbana-Champaign, 2004.
8. Yoon, H., Sheiretov, T., Cusano, C., "Tribological evaluation of some aluminum-based materials in lubricant/refrigerant mixtures," Wear 218 (1998) 54-65.
9. Erdemir, A., Eryilmaz, O. L., and Fenske, G., "Synthesis of diamondlike carbon films with superlow friction and wear properties," J. Vac. Sci. Technol. A, 18.4 (2000) 1987-1992.
10. Fontaine, J., Le Mogne, T., Loubet, J.L., and Belin, M., "Achieving superlow friction with hydrogenated amorphous carbon- some key requirements," Thin Solid Films, 482 (2005) 99– 108.
11. Garland, N.P., Hadfield, M., "Tribological analysis of hydrocarbon refrigerants applied to the hermetic compressor," Tribology International, 38 (2005) 732–739.
12. Kennedy, F.E., Lidhagen, D., Erdemir, A., Woodford, J. B., Kato, T., "Tribological behavior of hard carbon coatings on steel substrates," Wear, 255 (2003) 854–858.
13. Sheiretov, T., "Scuffing of Aluminum/Steel Contacts Under Dry Sliding Conditions," PhD. Thesis, University of Illinois, 1997.
14. MatWeb Online Materials Information Resource. http://www.matweb.com/ (last accessed 4/2/2006).
15. Meerkamm, H., Fruth, W., Krumpiegl, T., Schaufler, C., "Mechanical and tribological properties of PVD and PACVD wear resistant coatings," International Journal of Refractory Metal s& Hard Materials, 17 (1999) 201-208.
16. Wanstrand, O., Larsson, M., Hedenqvist, P., "Mechanical and tribological evaluation of PVD WC/C coatings," Surface and Coatings Technology, 111 (1999) 247–254.
17. Holmberg, K., Ronkainen, H., Matthews, A., "Tribology of thin coatings," Ceramics International, 26 (2000) 787-795.
18. Private communication with Dr. Ali Erdemir, Argonne National Laboratory, April 15, 2005.
19. Oliver, W.C., Pharr, G.M., "Measurement of hardness and elastic modulus by instrumented indentation: Advances in understanding and refinements to methodology," J. Mater. Res., 19 (2004) 3-20.
20. Guo, Y.B., Warren, A.W., "Microscale Mechanical Behavior of the Subsurface by Finishing Processes," Journal of Manufacturing Science and Engineering, 127 (2005) 333-338.
21. Gubisch, M., Liu, Y., Spiess, L., Romanus, H., Krischok, S., Ecke, G., Schaefer, J.A., Knedlik, Ch., "Nanoscale multilayer WC/C coatings developed for nanopositioning: Part I. Microstructures and mechanical properties," Thin Solid Films, 488 (2005) 132-139.

22. Fontaine, J., Belin, M., Le Mogne, T., Grill, A., "How to restore superlow friction of DLC-the healing effect of hydrogen gas," Tribology International, 37 (2004) 869–877.

23. TriboScope, Hysitron, Inc., Minneapolis, MN, http://www.hysitron.com/Products/ProductPages/products_triboscope.htm

24. Tayebi, N., Polycarpou, A. A., Conry, T. F., "Effects of substrate on determination of hardness of thin films by nanoscratch and nanoindentation techniques," J. Mater. Res., 19 (2004) 1791-1802.

25. Solzak, T., Polycarpou, A. A., IN PRESS, "Engineering Outreach to Cub Scouts with Hands-on Activities Pertaining to the Pinewood Derby Car Race," International Journal of Engineering Education.

26. Gargiulo, J., and Gargiulo, S., 2001, "Winning Pinewood Derby Secrets," 2nd ed. Trumbull, CT, accessed at http://www.pinewoodpro.com (September 2005).

27. J. Douglas, E. Iversen, and C. Kalyandurg, "Engineering in the K-12 Classroom: An Analysis of Current Practices & Guidelines for the Future," Production of the ASEE EngineeringK12 Center (November 2004).

28. Symans, M.D., "Introducing middle school students to engineering principles using educational bridge design software," Journal of Engineering Education, 89 (2000).

29. R. Speaks, Hands-on engineering for high school students. Proceedings of the 1998 Annual ASEE Conference (Seattle, WA, June 1998).

30. Bowden, F.P., Tabor, D., 1982, "Friction: An Introduction to Tribology," p. 91, Krieger Publishing Company, Malabar, Florida.

31. Ballou, J., Camis, S., Koo, S., Wait, K., 2005, "MIE470 Team 13: The Ultimate Pinewood Derby Car," Senior Design Project, University of Illinois at Urbana-Champaign.

32. Corr, D., Corr, B., 2004 "Pinewood Derby Speed Secrets: The Science of Speed," http://www.pinewoodprofessor.com/ (December 2005).

33. ABC Pinewood Derby, "Build a Winning Pinewood Derby Car," accessed at http://www.abc-pinewood-derby.com/design-pinewood-derby-car.htm (December 2005).

34. Pope, S., 2002, "Learn to Build a Winner," accessed at http://members.aol.com/standcmr/lbw_apl.html (January 2006).

35. Design-Expert 6, Stat-Ease, Inc., Minneapolis, MN, http://www.statease.com/.

Appendix A: Nanoindentation and Running-In Investigation

A.1 Nanoindentation Procedure

In order to validate manufacturer's specifications and determine the nanohardness and reduced modulus of the coatings tested, nanoindentation was performed using a Hysitron TriboScope® fitted to a MultiMode AFM. A view of the TriboScope is given in Figure A.1. A detailed review of the nanoindetation method is given by Oliver and Pharr [19].

Figure A.1: Hysitron TriboScope® [23]

Two of the most commonly used loading profiles are triangle and pull-loading. Triangle involves applying a specified load at a constant rate and immediately unloading at that same rate. An example of this profile is depicted in Figure A.2. Pull-loading is similar to a set of smaller triangle load profiles. A maximum load is specified and divided into 10 steps as shown in Figure A.3. After each successively higher load is applied, the transducer is partially unloaded, allowing the determination of hardness and reduced modulus at various depths. Care must be taken, though, to ensure that work hardening is not occurring during each load step. This is accomplished by first performing triangle-load indentations at various depths and comparing the results to those obtained with a pull-loading indentation. If they are similar, then it is assumed that work hardening can be neglected. In this investigation, after performing several triangle-load indentations at loads up to 8 mN, pull-loading was used with a maximum load of 6 mN. Loading (and unloading) rates of 800 µN/s and 1200 µN/s were used for 4000 µN and 6000 µN indentations for both triangle and pull-load profiles. One thousand data points were acquired for triangle-load, while 8000 points were acquired for pull-load indentations due to the increase in load intervals. Representative load-depth plots are depicted in Figures A.4 and A.5.

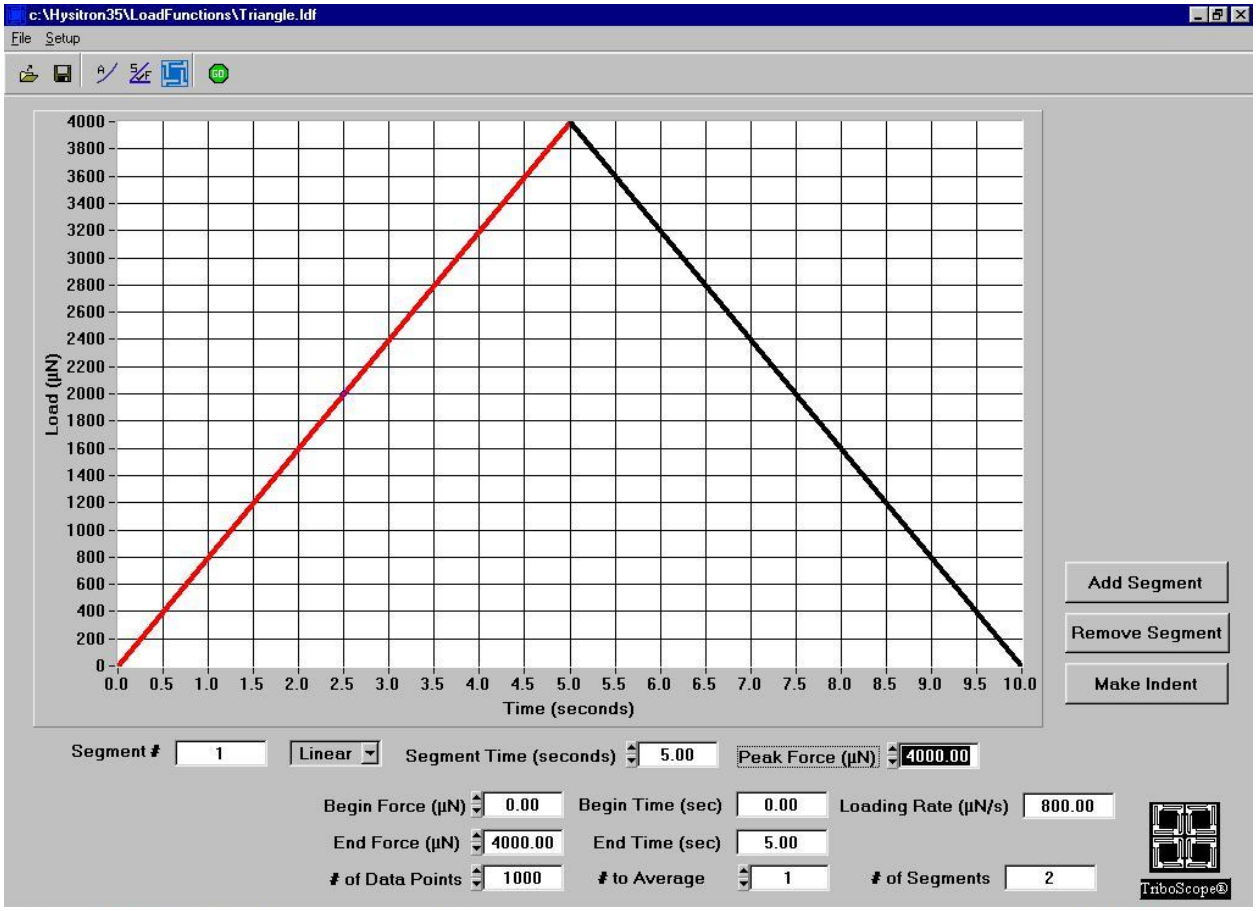

Figure A.2: Triangle-load profile

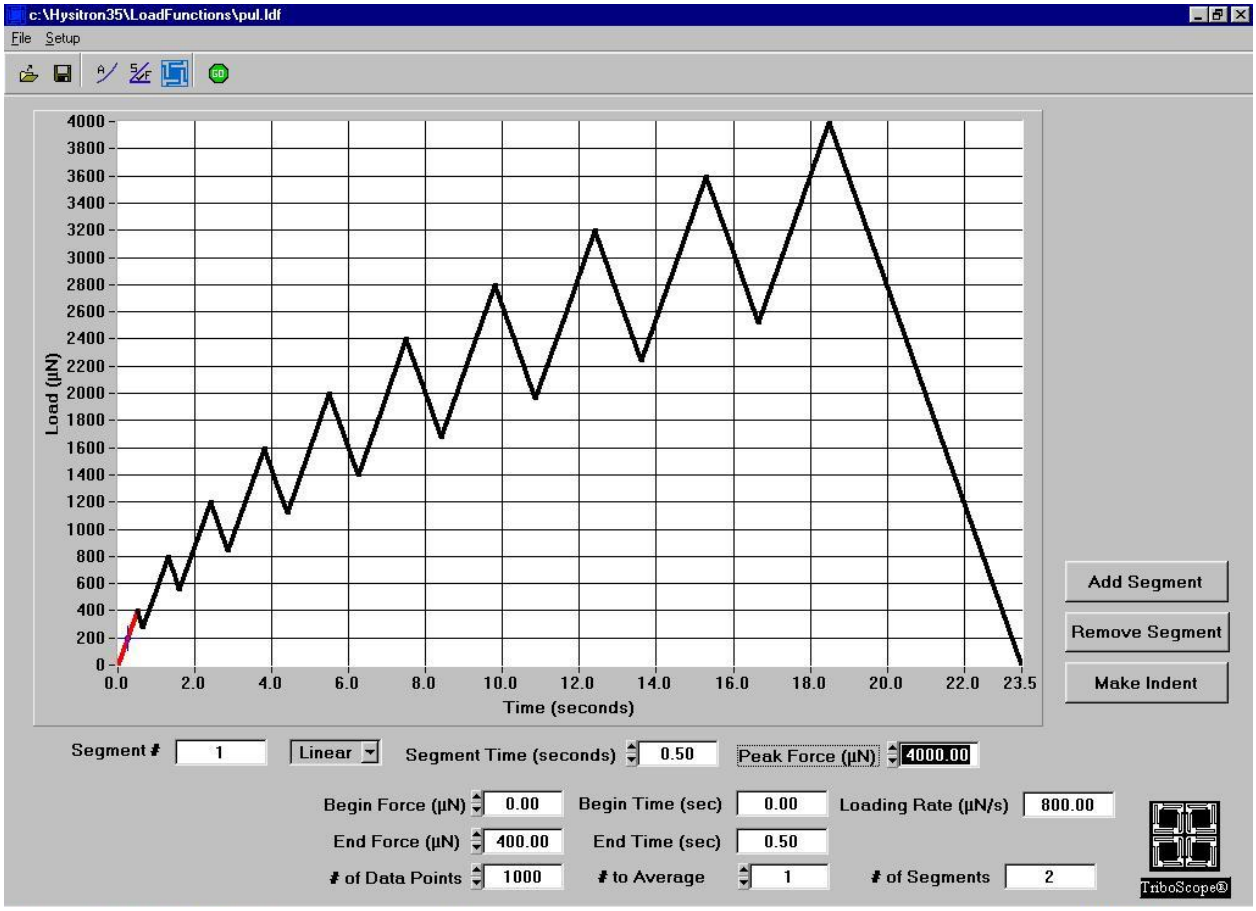

Figure A.3: Pull-load profile

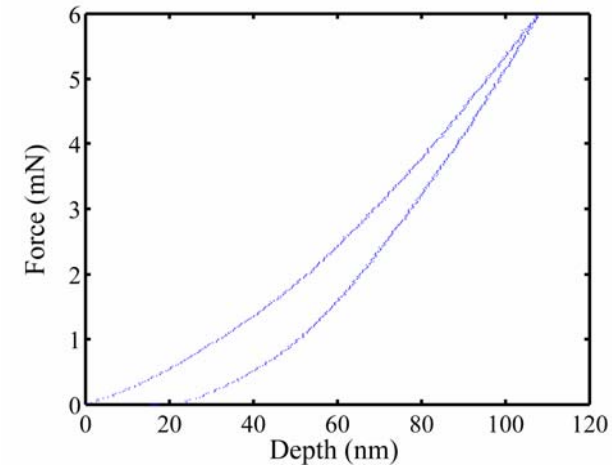

Figure A.4: Representative load-depth plot for triangle-load profile

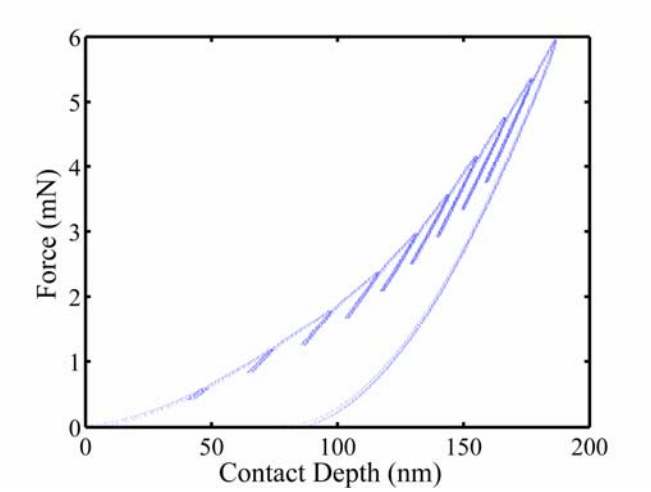

Figure A.4: Representative load-depth plot for pull-load profile

There are many different indenter tip geometries that can be used but are usually suited to a particular type of material or depth. Here, a relatively sharp Berkovich tip (triangular pyramid) was used that is accurate at contact depths ranging from 50-200 nm. Loads were chosen to obtain a depth slightly less than the maximum.

A.2 Virgin Samples

Nanoindentation was performed on uncoated and coated 52100 steel pins in this research, and hardness and reduced modulus values are provided in Section 2.4. Values for uncoated A390-T6 were obtained from Pergande and Polycarpou [3]. It is assumed that properties of the coatings on the steel pins are similar to those on A390-T6, which is reasonable as the penetration of the coating was about 10% of the thickness, less than the limit of 20% to avoid substrate effects [24]. It is also assumed that the influence of pin curvature on the properties could be neglected due to the large differential between the pin and tip radii. It was necessary, however, to indent normal to the pin surface for accurate measurements.

Hardness and reduced modulus plots for uncoated, WC/C(A), WC/C + DLC coated pins are shown in Figure A.5. Nanoindentation was not performed on WC/C(B), but is assumed to be similar to WC/C(A). The reasons for anomalies in some of the plots are unknown, but hardness and modulus values for different indentations are very similar for the most part. Important to note is that the uncoated pin hardness is higher than the bulk hardness of ~7.3 GPa (converted from 62 HRC), and is actually higher than WC/C(A), suggesting that improvement in wear is a result of differences in surface energies of the contacting materials. Also, the properties for the WC/C + DLC coating reflect only those of the DLC coating as the DLC overcoat is penetrated less than 5%.

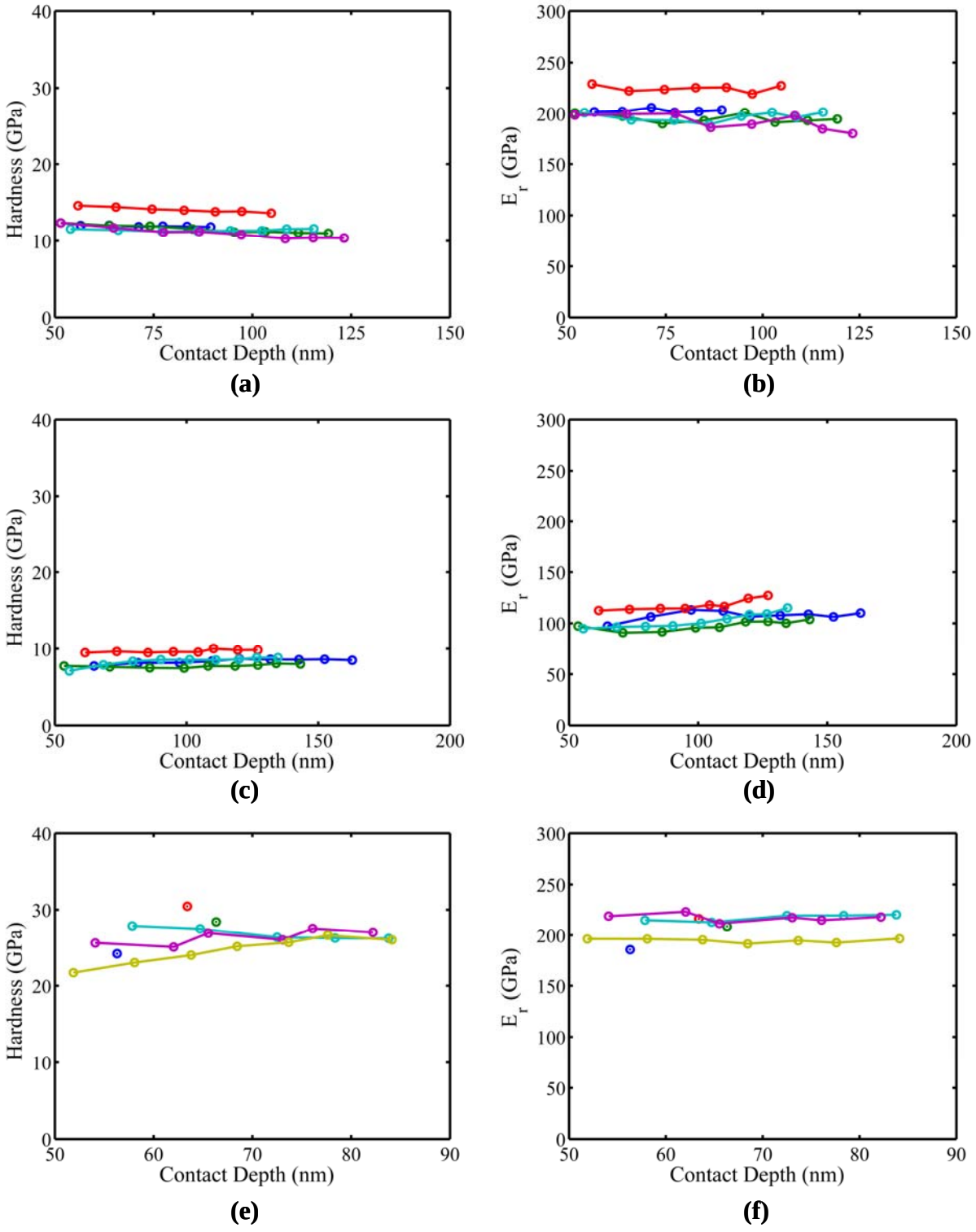

Figure A.5: Hardness and reduced modulus of virgin (a-b) Uncoated, (c-d) WC/C(A), and (e-f) WC/C + DLC coated pins obtained with a maximum load of 6 mN

A.3 Worn WC/C(A): Running-in Investigation

It was hypothesized that work-hardening of the WC/C(A) coating may occur during testing at elevated temperatures due to the high friction produced in the running-in period. This would explain the resulting lower steady-state friction coefficient values as compared to lower temperature tests. To test this, nanoindentation was performed pins from the 5 minute, 10 minute, and 21 minute tests with indentations in the center and edge of wear on the pin, as illustrated by the white X in Figure A.6.

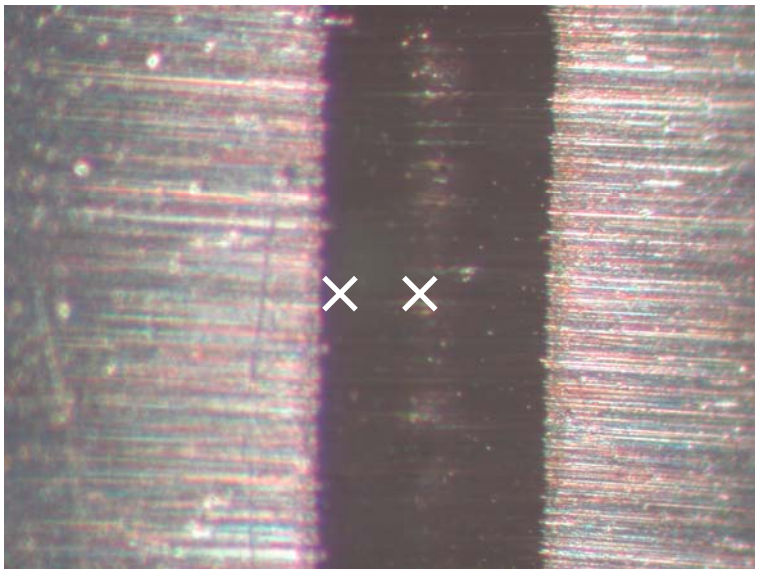

Figure A.6: Nanoindentation locations

Hardness and reduced modulus values are plotted in Figure A.7 at various depths. After 5 minutes, values are relatively consistent and slightly higher than virgin values with a hardness of 12.5-14.5 GPa. This suggests that there may be some work-hardening of the coating in the first 5 minutes. After 10 minutes, the hardness increases further with values up to 19 GPa at the center of wear, but more scatter in the data is observed. However, as can be seen in Figure A.8, the thickness of the WC/C coating in one portion of the wear is only ~.5 μm, meaning the contact depth is 17% of the thickness of the coating. The reduced modulus values approach those of the substrate meaning substrate effects cannot be neglected. Interesting to note, though, is that the hardness is higher than that of virgin 52100 steel, possibly due to work hardening itself. The hardness and reduced modulus values at 21 minutes are similar to those at 5 minutes because there is slightly less wear than in the 10 minute test, exhibited in Figure A.9. Based on these observations, work hardening of the coating is most likely not the cause of the lower friction after running-in, but the higher virgin hardness of the 52100 steel substrate and apparent work hardening exhibited in the 10 minute test may contribute.

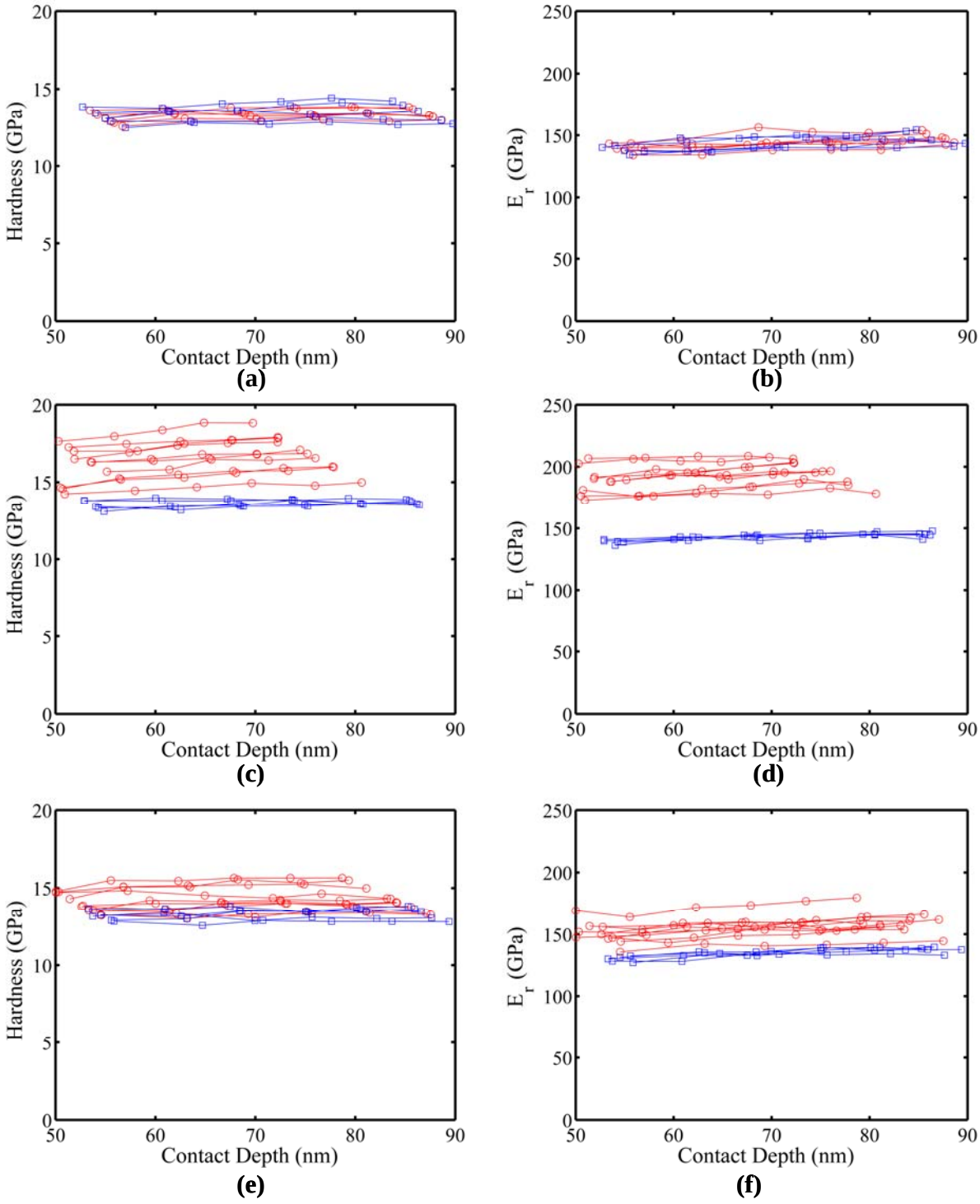

Figure A.7: Hardness and reduced modulus for running-in specimens after (a-b) 5 minutes, (c-d) 10 minutes, and (e-f) 21 minutes obtained with a maximum load of 4 mN. Red data points are those obtained in the center of the wear and blue were obtained at the edge of wear.

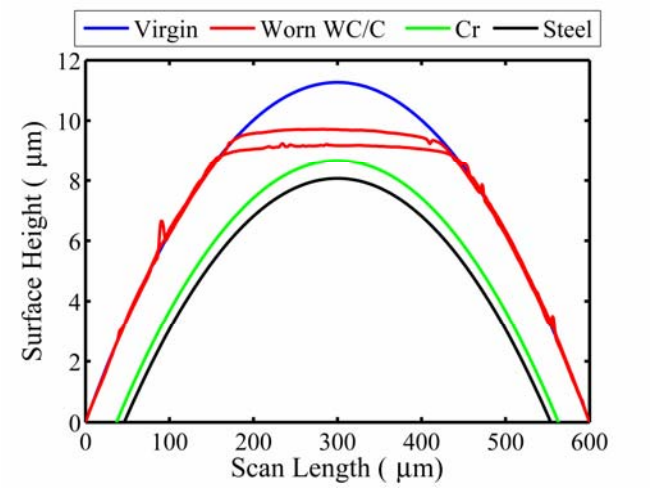

Figure A.8: Wear scans (red) of the 10 minute running-in test with Cr underlayer and steel substrate references

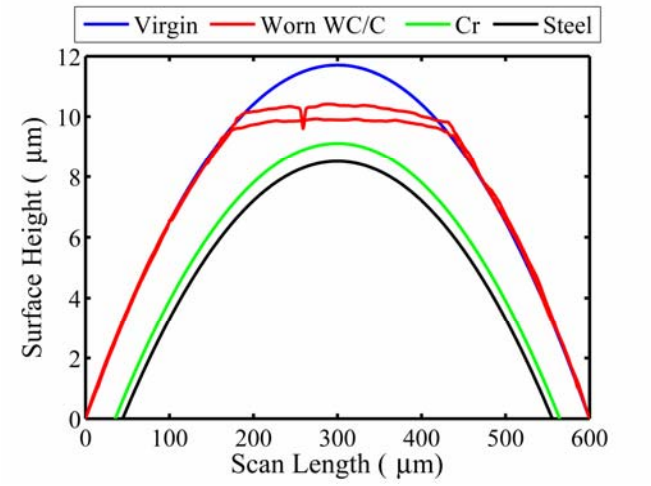

Figure A.9: Wear scans (red) of the 21 minute running-in test

Appendix B: Contact Profilometry

All roughness and were measurements were completed with the Tencor P-15 Profiler, pictured in Figure B.1. A load of 5 mg was applied with a 2.5 µm stylus tip. General roughness measurements of virgin uncoated and coated samples were performed perpendicular to machining marks (see Figures 2.12 and 2.35 for machining marks) with a length of 2 mm, speed of 50 µm/s, and sampling frequency of 500 Hz for a total of 20000 data points to obtain the most accurate profile. A sample roughness scan of a cast iron disk is shown in Figure B.2.

Figure B.1: Tencor P-15 Profiler in Microtribodynamics Laboratory

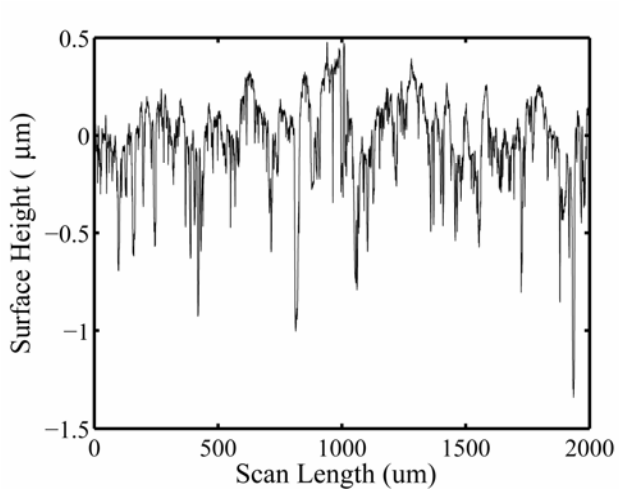

Figure B.2: Sample roughness scan of a cast iron disk (Rq = 235 nm)

Wear scans require much less data points and, thus, were performed at a speed of 100 µm/s and sampling rate of 100 Hz. For pins, a scan length of 800 µm was used, oriented parallel to the sliding direction as shown in Figure 2.35. Scans of worn disks were performed with a length of 12 mm perpendicular to the wear track. Wear on both coated A390-T6 and cast iron disks was generally not distinguishable from the roughness (except for scuffing tests), and only two scans of each were taken.

For the running-in investigation of WC/C(A)-coated pins on cast iorn, roughness scans were also performed to find a correlation between roughness and running-in. In this case, scans were taken perpendicular to the sliding direction. During the hardness investigation, it was discovered that a significant micro-roughness was apparent on virgin and 21 minute tests while 5 minute tests had little micro-roughness. To capture this micro-roughness, a scan speed of 20 µm/s and sampling rate of 500 Hz were used with a scan length of 4 mm in the center of the wear on pins and disks for a total of 100000 data points (see Figures 3.39 and 3.40).